地球惑星観測・探査学／惑星探査学2
「惑星大気の光学リモートセンシング」
Optical remote sensing of planetary atmospheres

新領域創成科学研究科　複雑理工学専攻
今村　剛
Takeshi Imamura
t_imamura@edu.k.u-tokyo.ac.jp

Understanding the diversity of planetary atmospheric environment

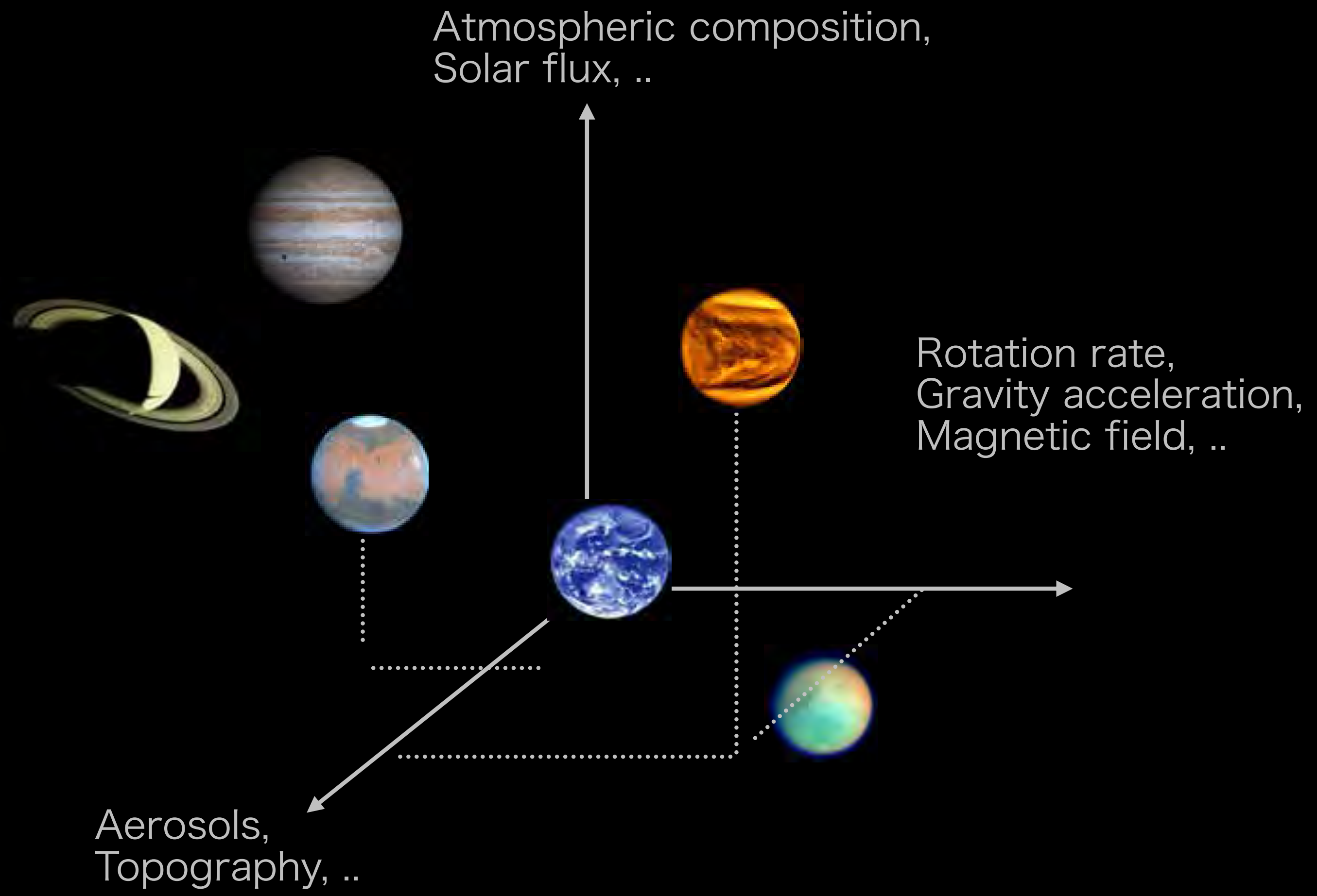

Composition of planetary atmospheres

Object	Mass (kilograms)	Carbon Dioxide	Nitrogen	Oxygen	Argon	Methane	Sodium	Hydrogen	Helium	Other
Sun	3.0×10^{30}							71%	26%	3%
Mercury	1000			42%			22%	22%	6%	8%
Venus	4.8×10^{20}	96%	4%							
Earth	1.4×10^{21}		78%	21%	1%					<1%
Moon	100,000				70%		1%		29%	
Mars	2.5×10^{16}	95%	2.7%		1.6%					0.7%
Jupiter	1.9×10^{27}							89.8%	10.2%	
Saturn	5.4×10^{26}							96.3%	3.2%	0.5%
Titan	9.1×10^{18}		97%			2%				1%
Uranus	8.6×10^{25}					2.3%		82.5%	15.2%	
Neptune	1.0×10^{26}					1.0%		80%	19%	
Pluto	1.3×10^{14}	8%	90%			2%				

photosynthesis

$$6\ CO_2 + 6H_2O + \text{energy} \longrightarrow C_6H_{12}O_6 + 6\ O_2$$

Vertical temperature profiles of planetary atmospheres

(Mueller-Wodarg et al.)

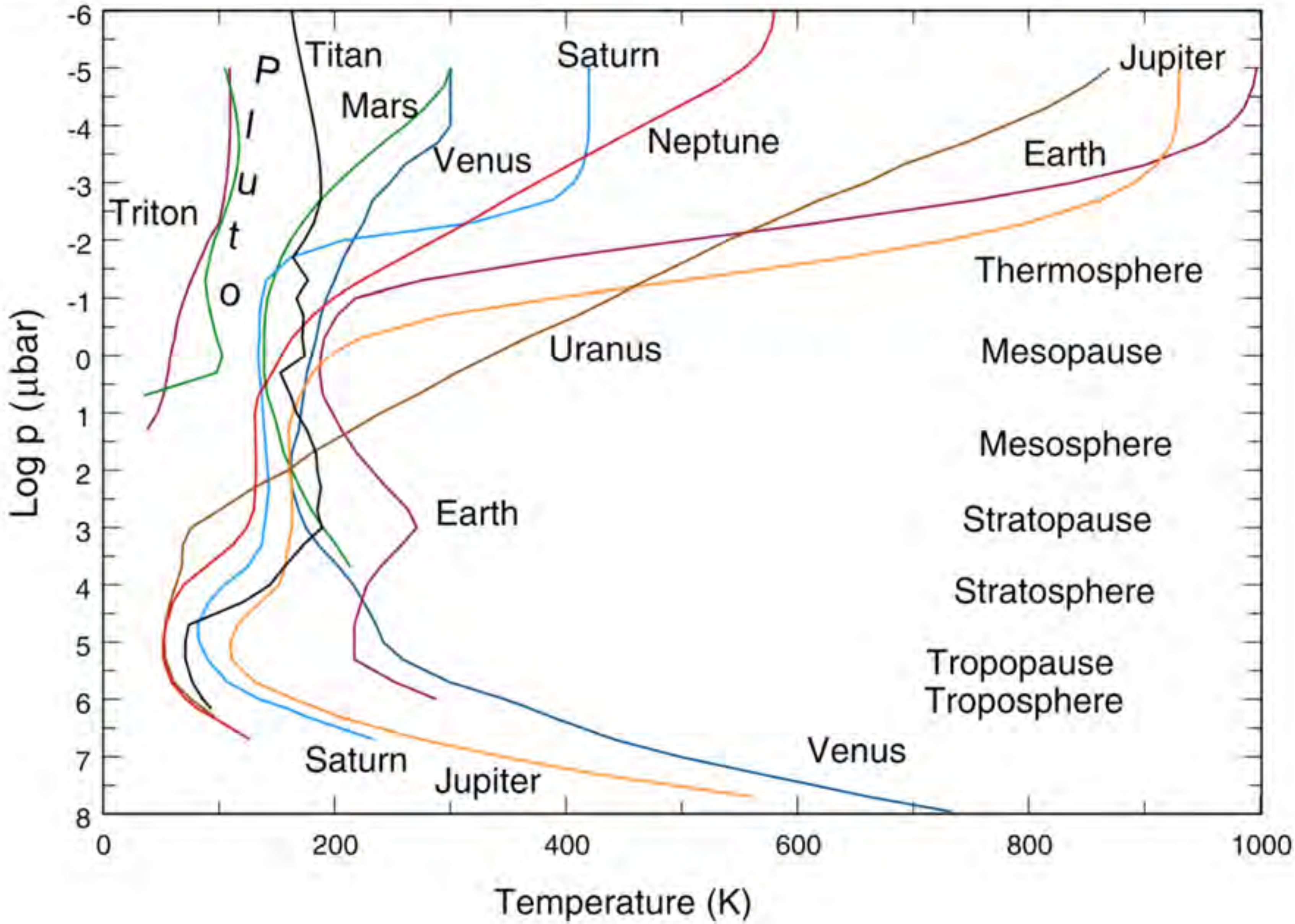

Jupiter

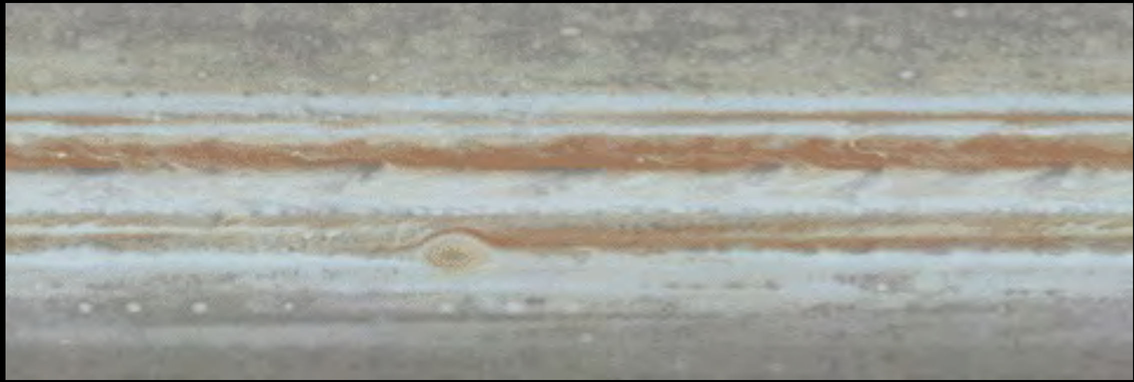

Earth

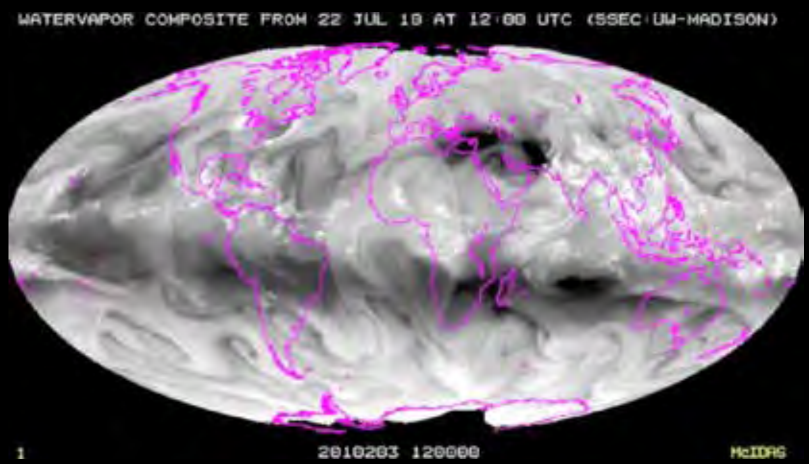

Venus

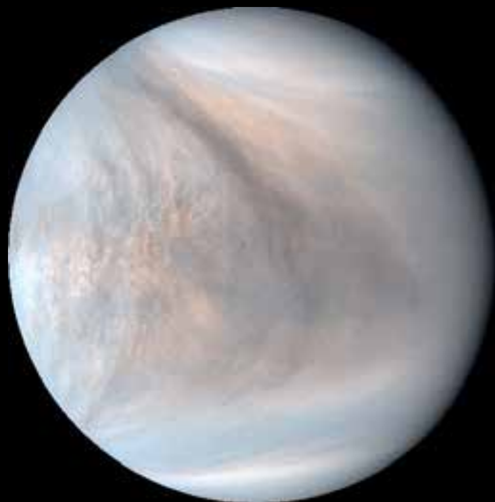

The atmosphere is not stationary. Continuous 3-D observation is essential.

Merits and demerits of observation methods

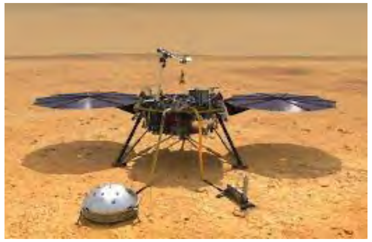

	Lander	Orbiter	Ground-based telescope
Spatial coverage	Limited	Global	Global
Time coverage	Short in many cases	Long & continuous	Repeatable
Observable variables	- In-situ measurements of gases and rocks - Many options	- Optical/radio remote sensing - In-situ plasma measurements	- Optical/radio remote sensing - Instruments can be large and new

Recent/future remote sensing missions

Venus Express

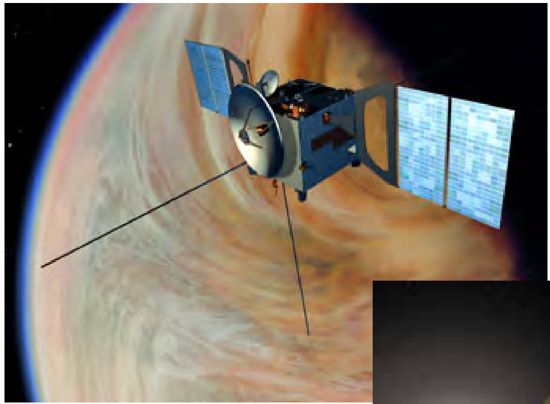

Mars Reconnaissance Orbiter

JUNO

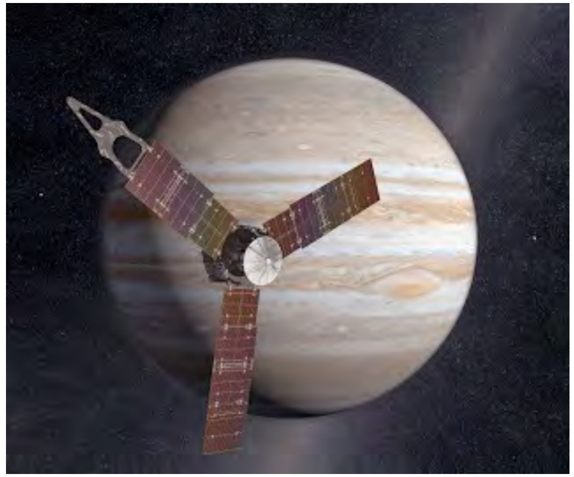

Akatsuki

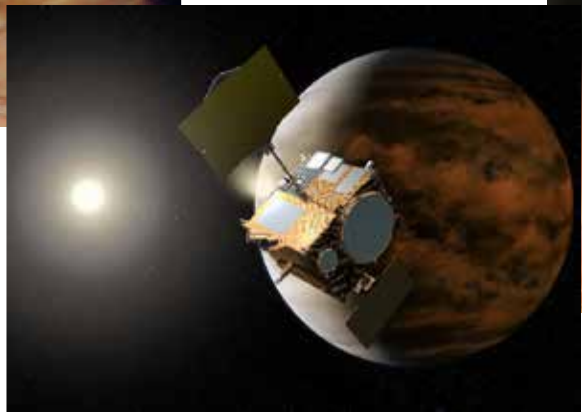

MMX

ExoMars Trace Gas Orbiter

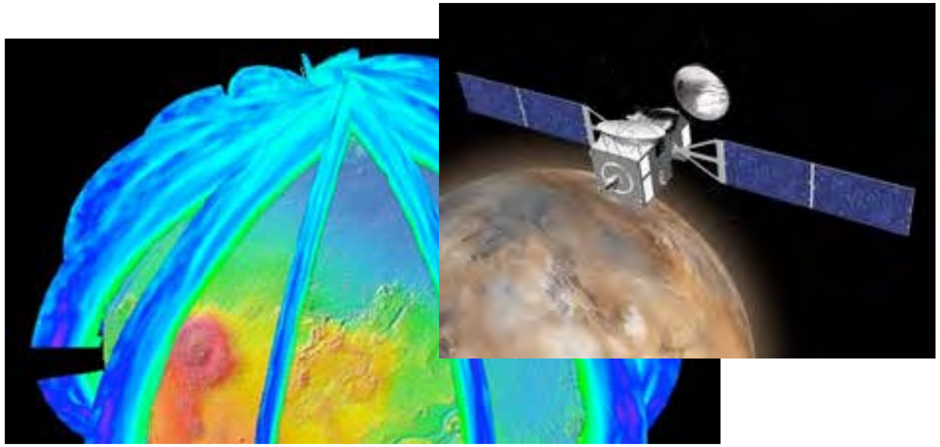

JUICE

Interaction between electromagnetic waves and molecules

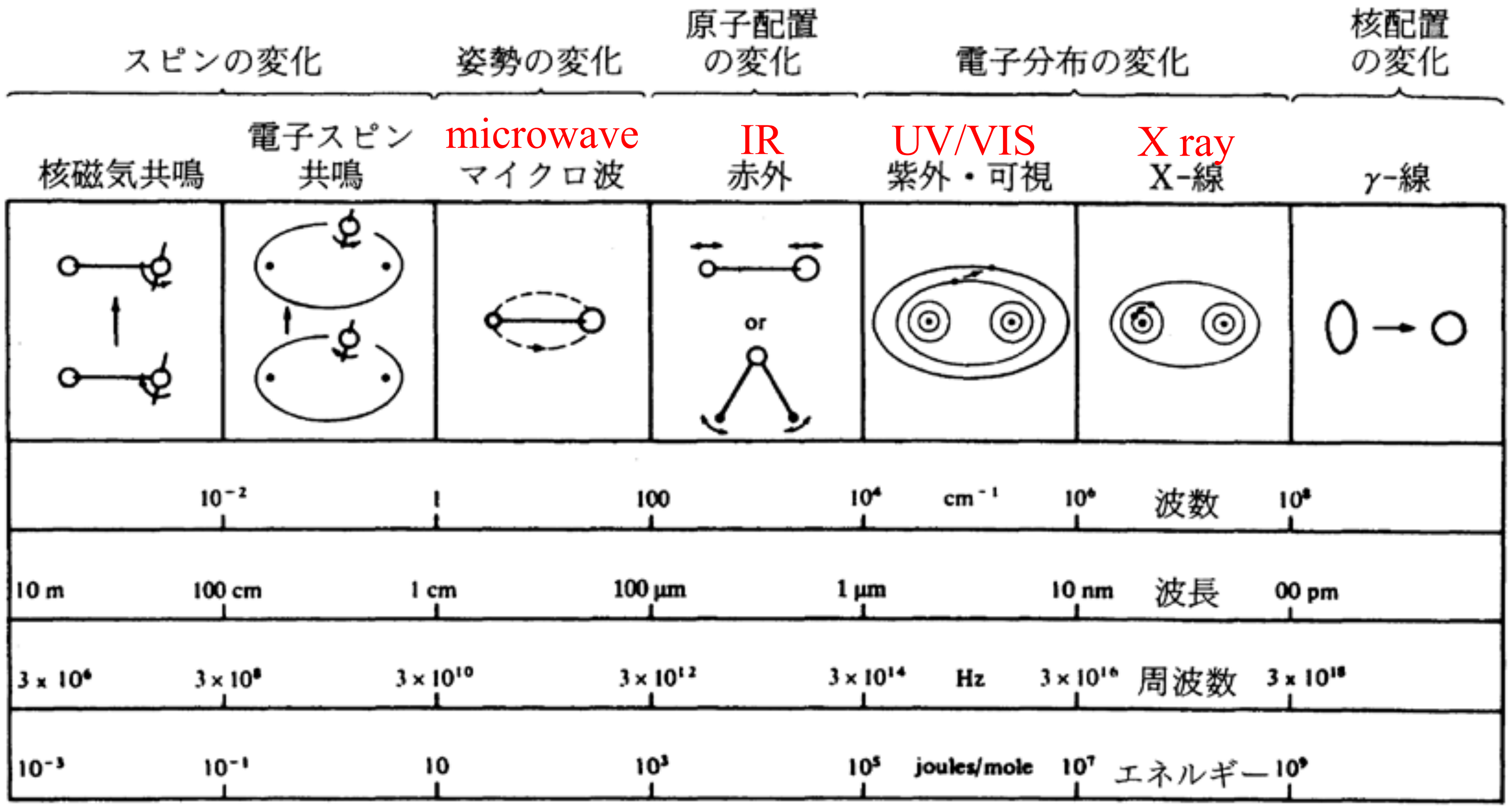

図 5.1 電磁波のスペクトルと電磁波–分子 (原子) の相互作用のメカニズム (Banwell and McCash, 1994)[26]

柴田（1999）

Molecular absorption

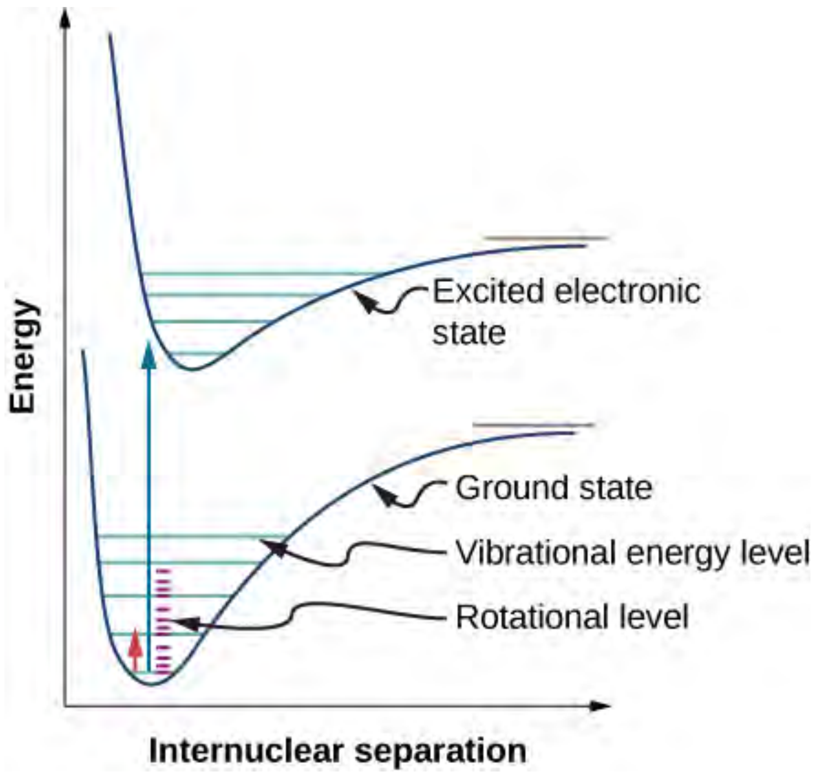

(LibreTexts libraries)

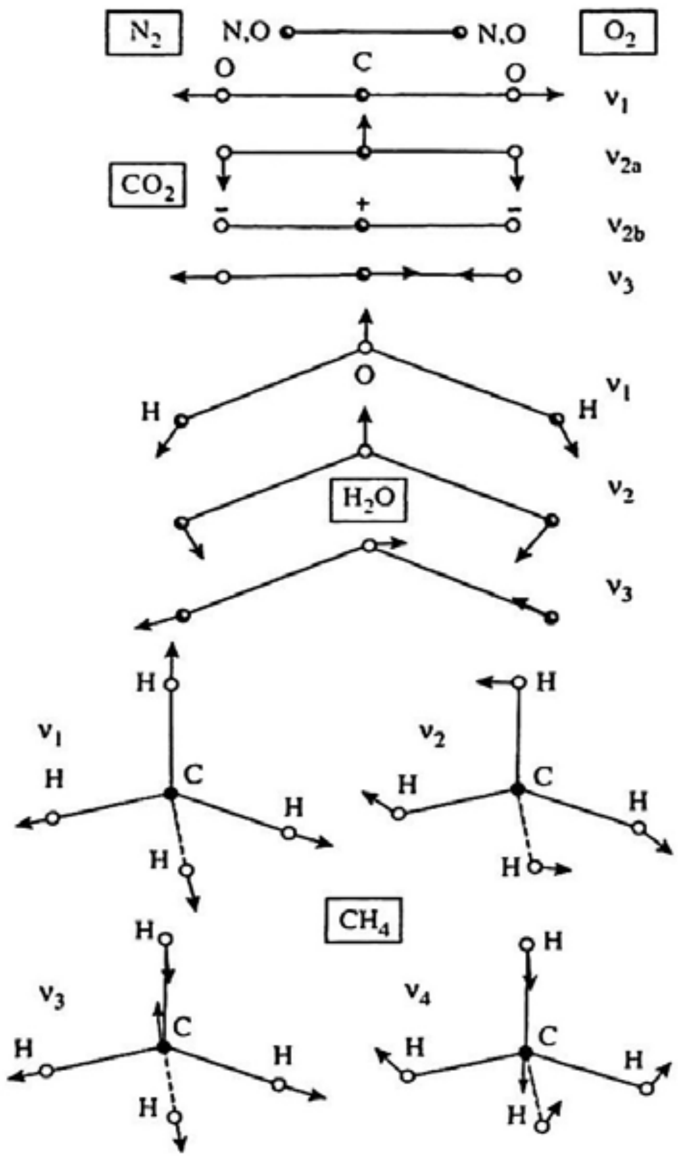

Catling & Kasting (2017)

Catling & Kasting (2017)

Vibrational energy levels

$$E_v = h\nu_0\left(v + \frac{1}{2}\right)$$

v : vibrational quantum number

Rotational energy levels

$$E_J = hB(J(J+1))$$

J : rotational quantum number

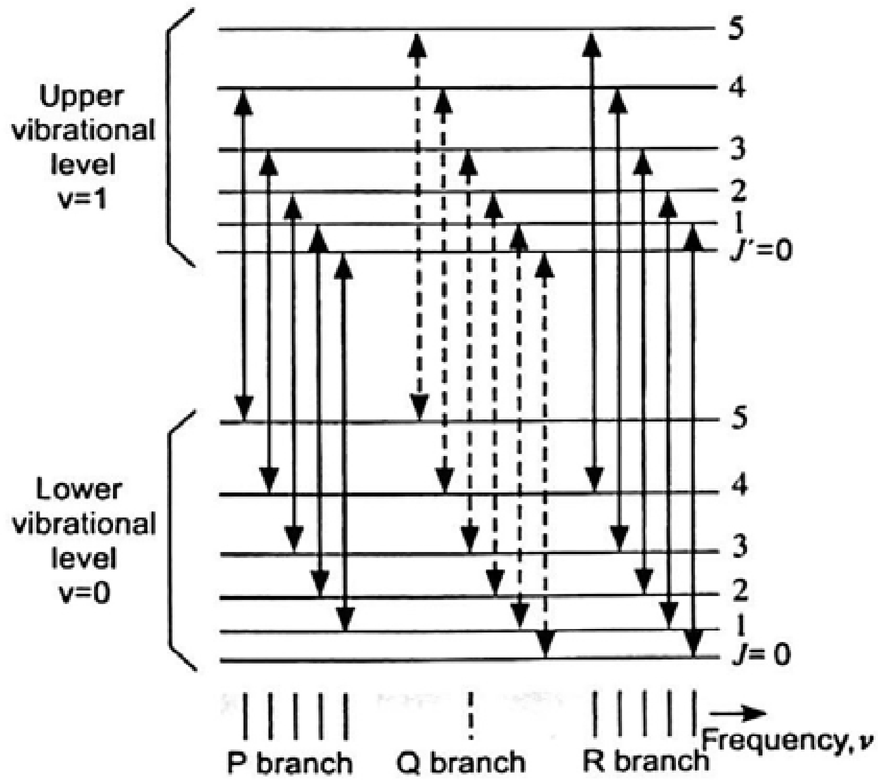

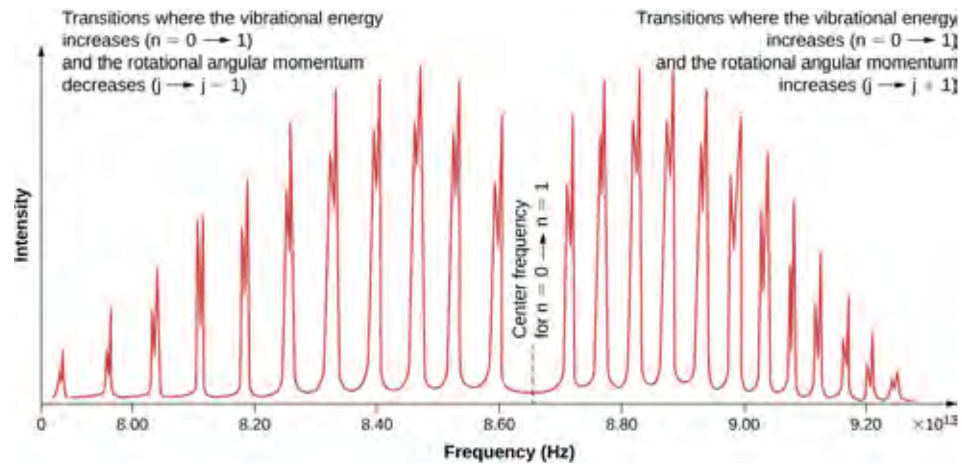

(LibreTexts libraries)

Line shape

Andrews (2010)

Extinction coefficient

line-shape function

$$k_\nu = \sum_n S_n f_n(\nu - \nu_n)$$

line strength

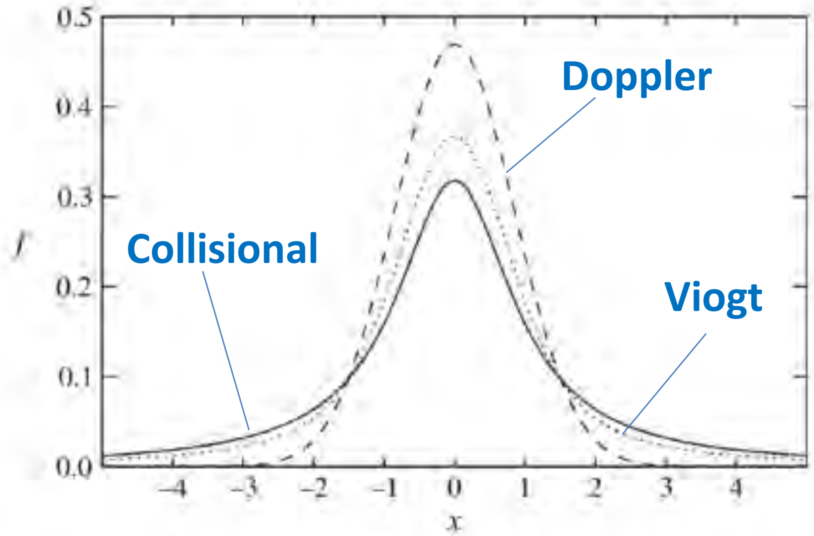

Illustrating the Lorentz (solid), Doppler (dashed) and Voigt (dotted) line shapes as a function of $x = (\nu - \nu_0)/\alpha$, where α is the half-width at half maximum appropriate for each shape. The curves are normalised such that the area under each is the same.

Collisional broadening

$$f(\nu - \nu_n) = \left(\frac{\gamma_L}{\pi}\right) \frac{1}{(\nu - \nu_n)^2 + \gamma_L^2}$$

$$\gamma_L \propto \boxed{p}\, T^{-1/2}$$

Dominant in the lower atmosphere

Doppler broadening

$$k_\nu = \frac{S}{\gamma_D \sqrt{\pi}} \exp\left(-\frac{(\nu - \nu_0)^2}{\gamma_D^2}\right)$$

$$\gamma_D = \frac{\nu_0}{c} \left(\frac{2k_B \boxed{T}}{m}\right)^{1/2}$$

Dominant in the upper atmosphere

Infrared spectra of the planets

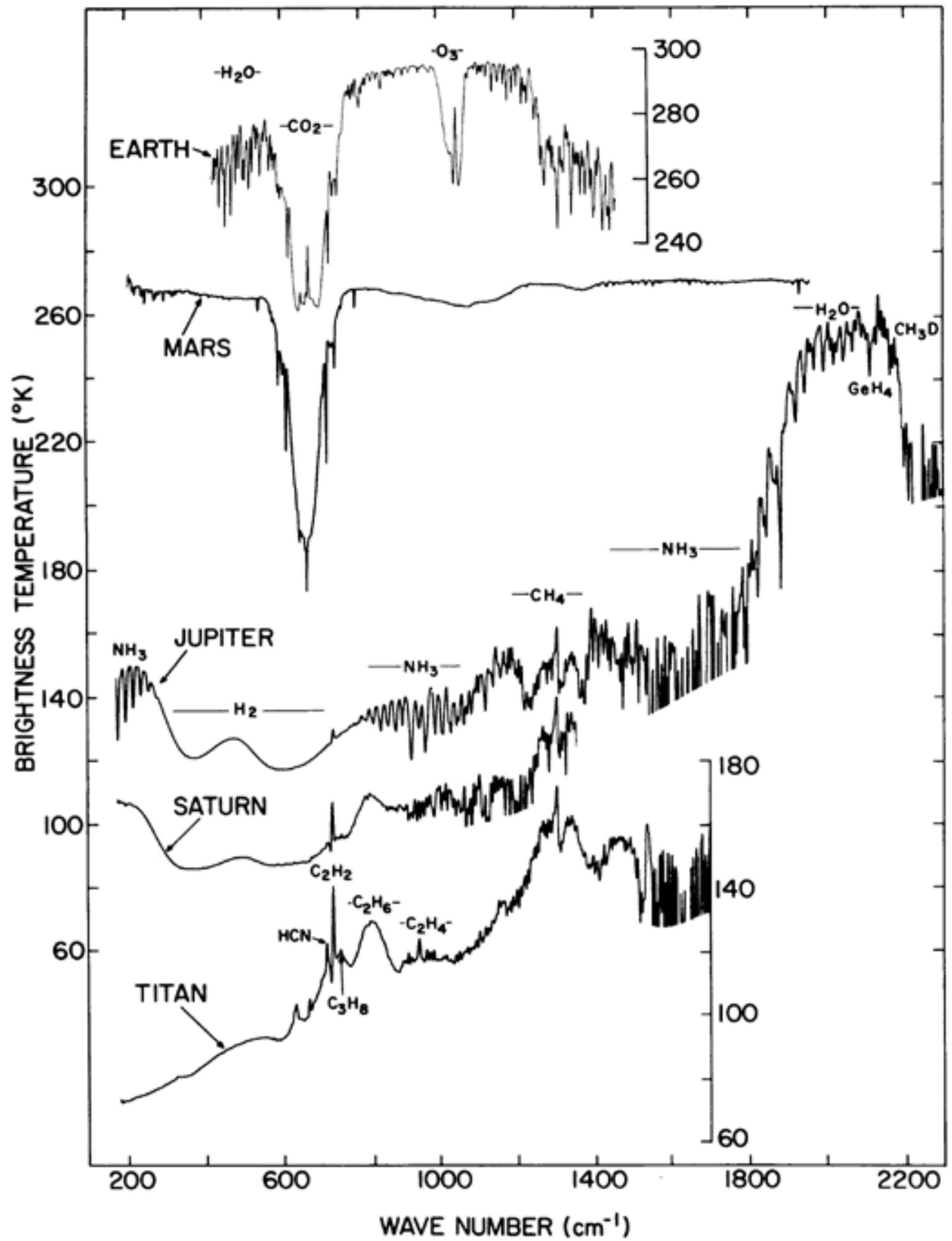

Fig. 4.21 Spectra in the thermal infrared, plotted as brightness temperatures, for four planets and Titan. Features that show as "absorptions" are formed in a region of negative temperature gradient (troposphere); those that show as "emissions" are from a warm stratosphere. [After HANEL (1983).]

Chamberlain & Hunten (1987)

Remote sensing of planetary atmospheres

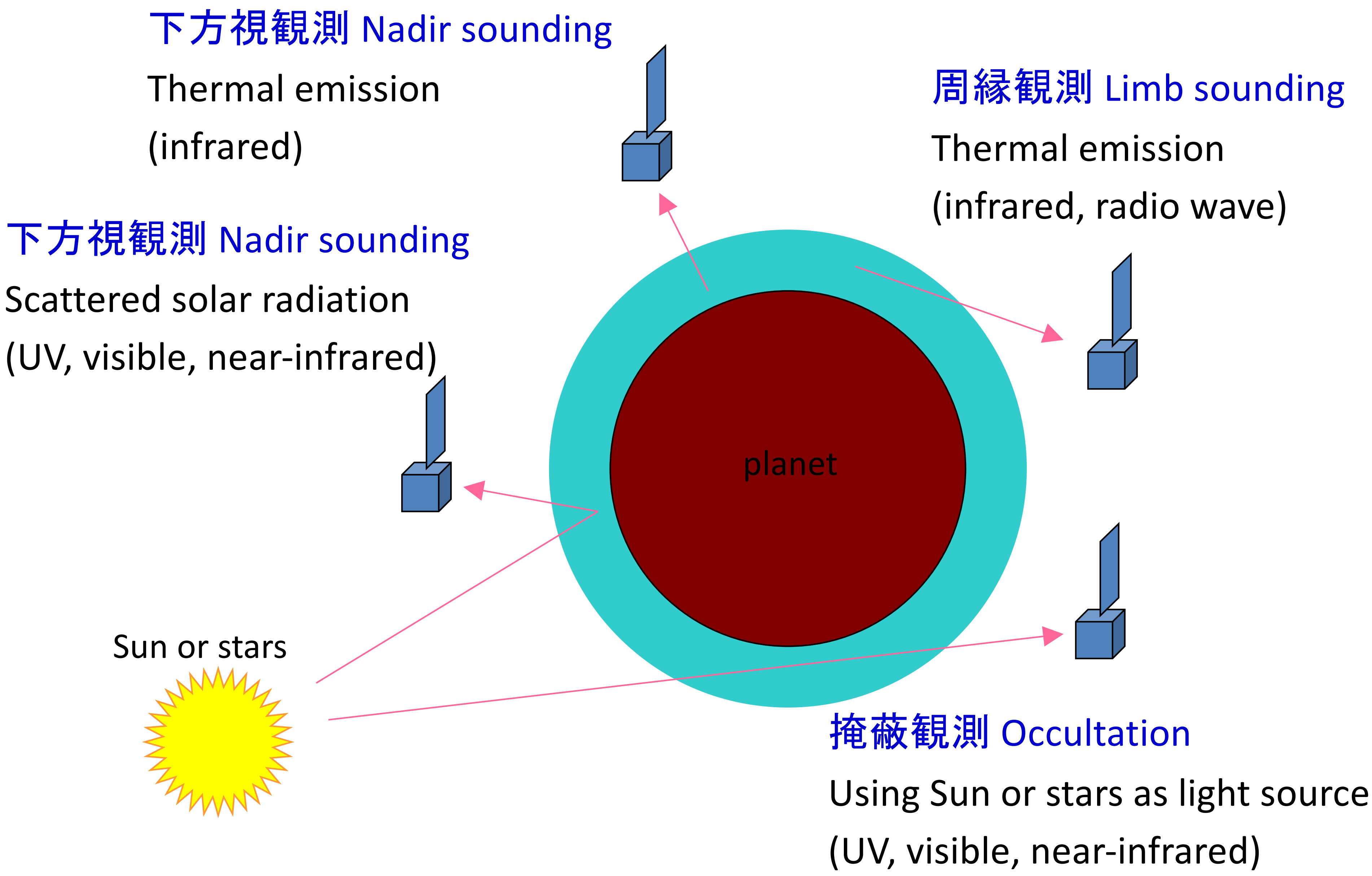

Spectroscopy

Grating spectrometer

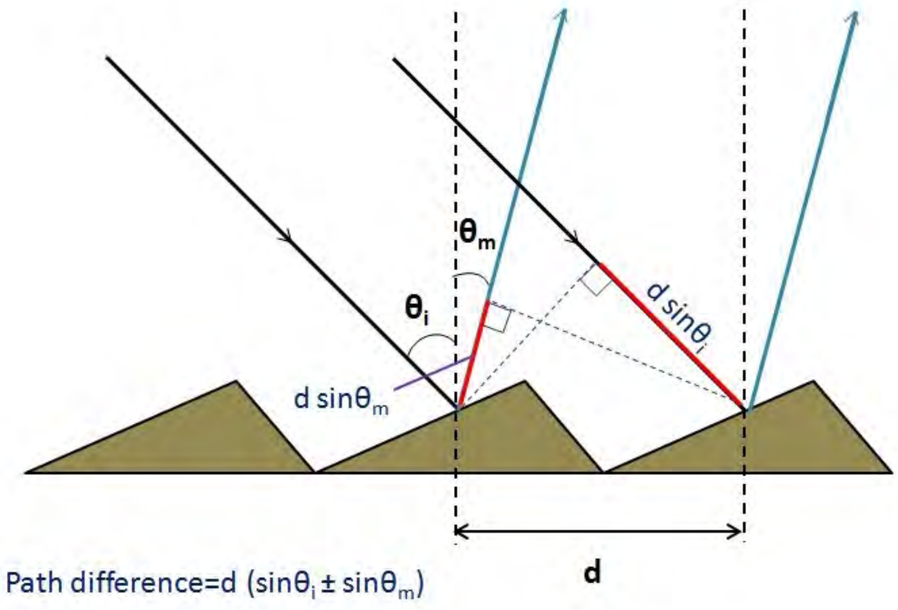

From Wikipedia

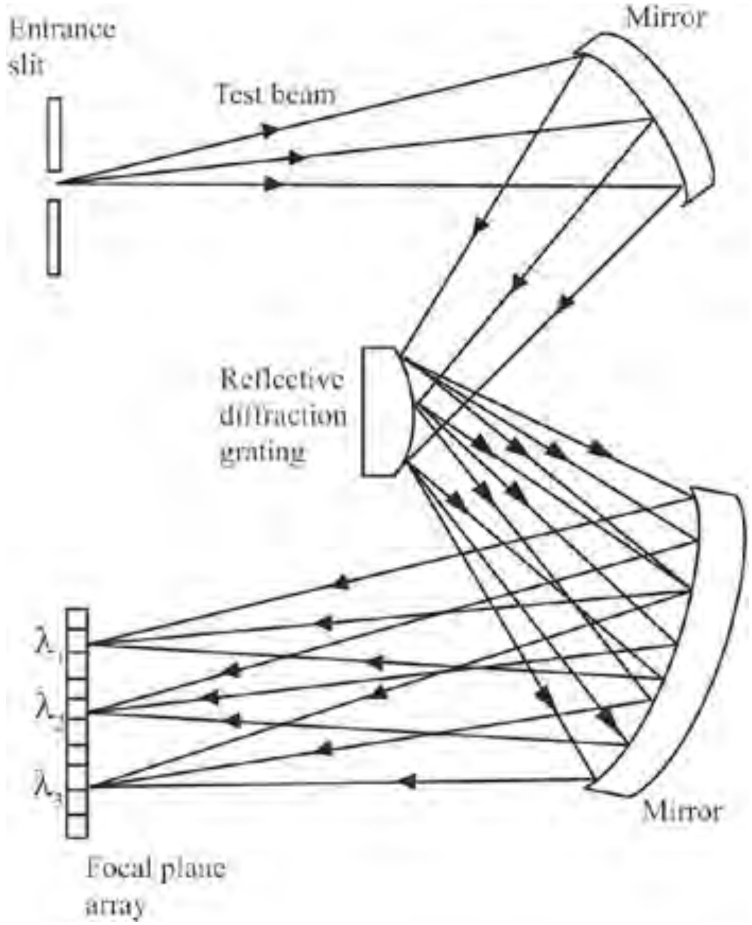

Crawford (2007)

Fourier spectrometer

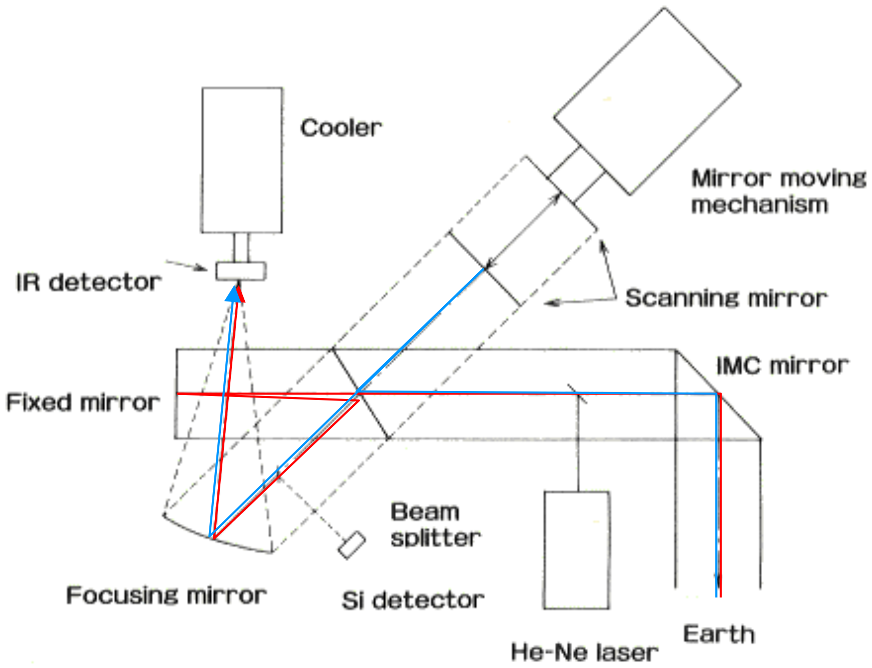

ADEOS/IMG Optical System

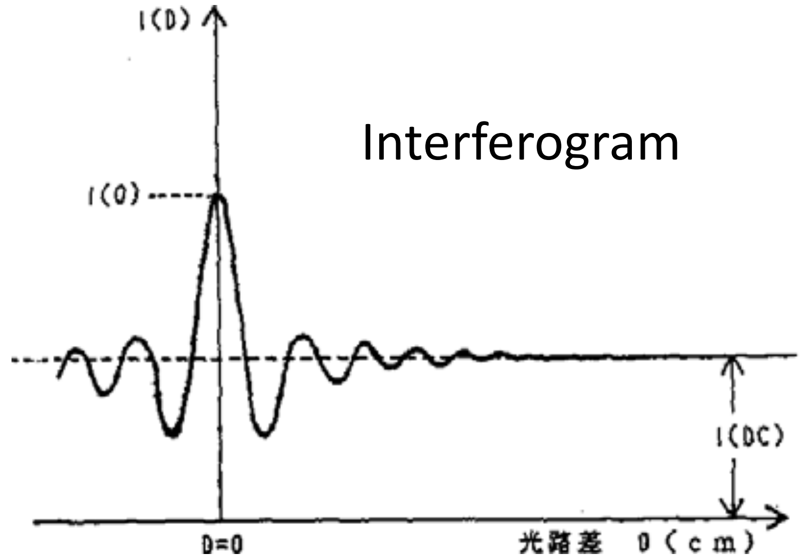

Interferogram

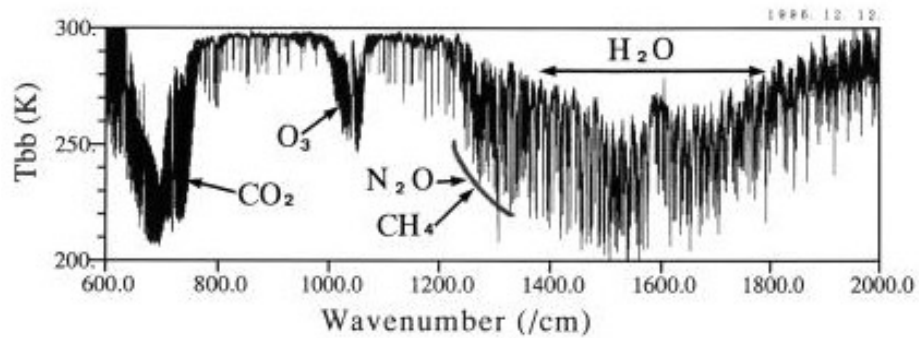

Interferogram →(FFT)→ Spectrum

* High spectral resolution for long scanning length

Solar occultation

strong light source → high S/N

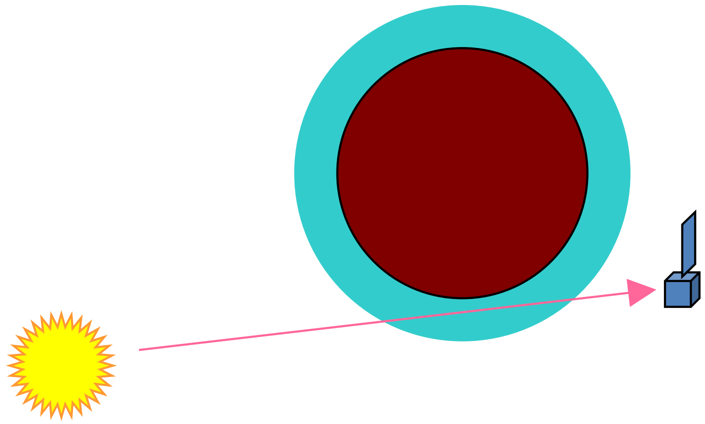

Solar occultation spectrum of Mars atmosphere recorded by ExoMars Trace Gas Orbiter/ACS Mid-IR channel (at 5.5 km altitude)

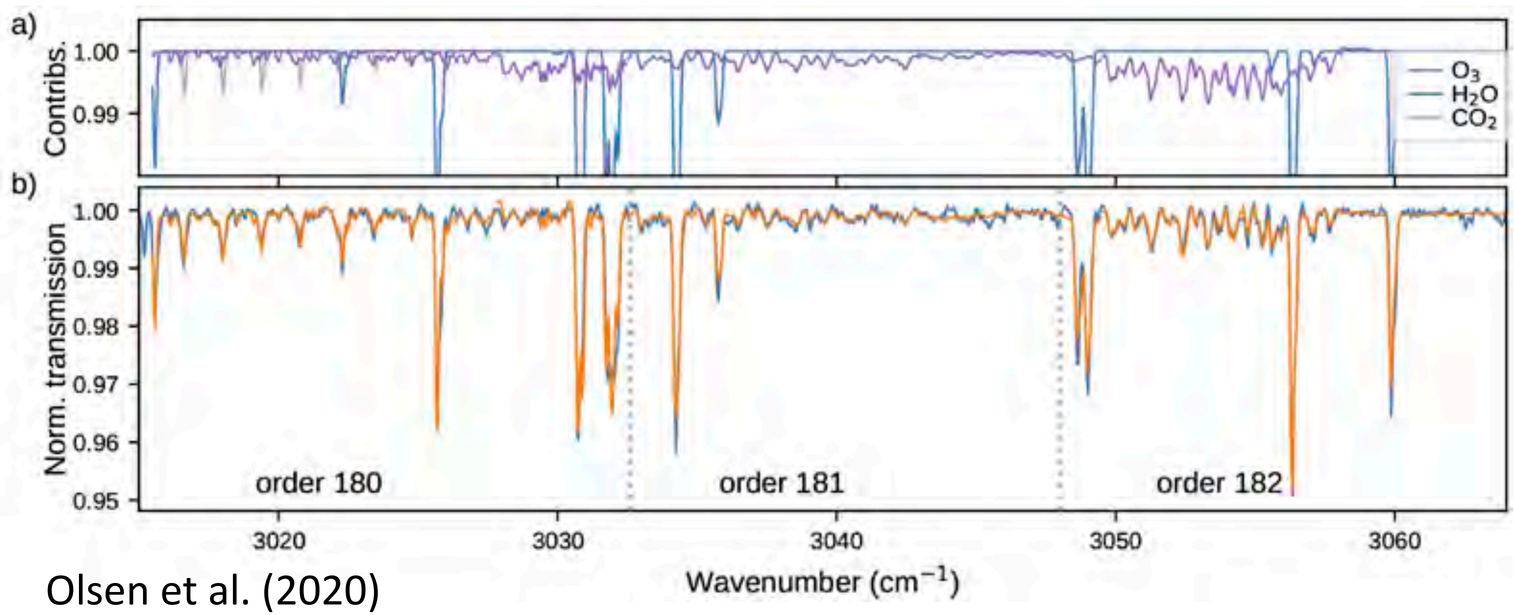

contributions from O_3, H_2O, and CO_2 to the best-fit

data and best-fits

Olsen et al. (2020)

Solar occultation by Venus Express/SPICAV-SOIR

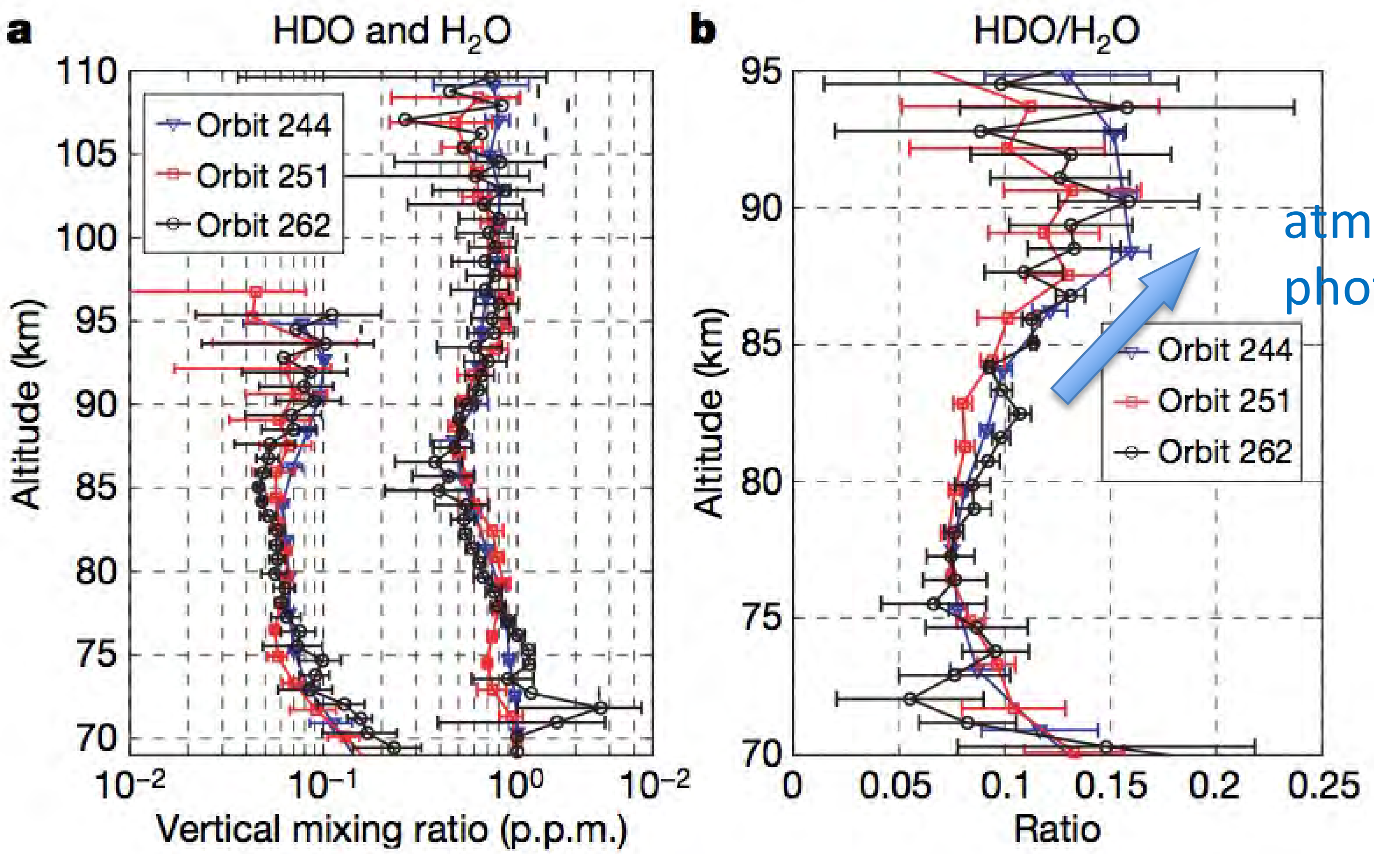

atmospheric escape?
photochemistry?

Bertaux et al. (2007)

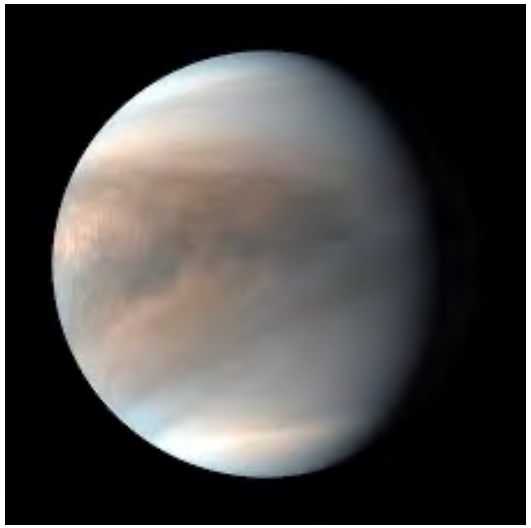

SO, SO_2 profiles above clouds observed by Venus Express solar occultations (Belyaev et al. 2012)

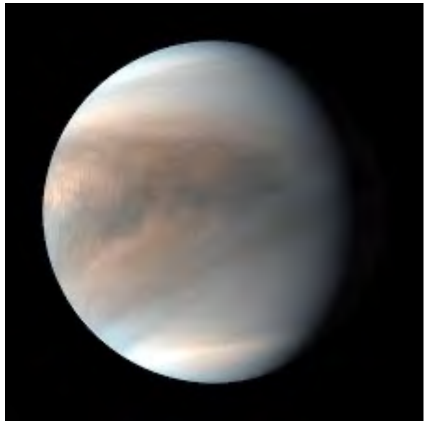

SO: black

SO_2: blue

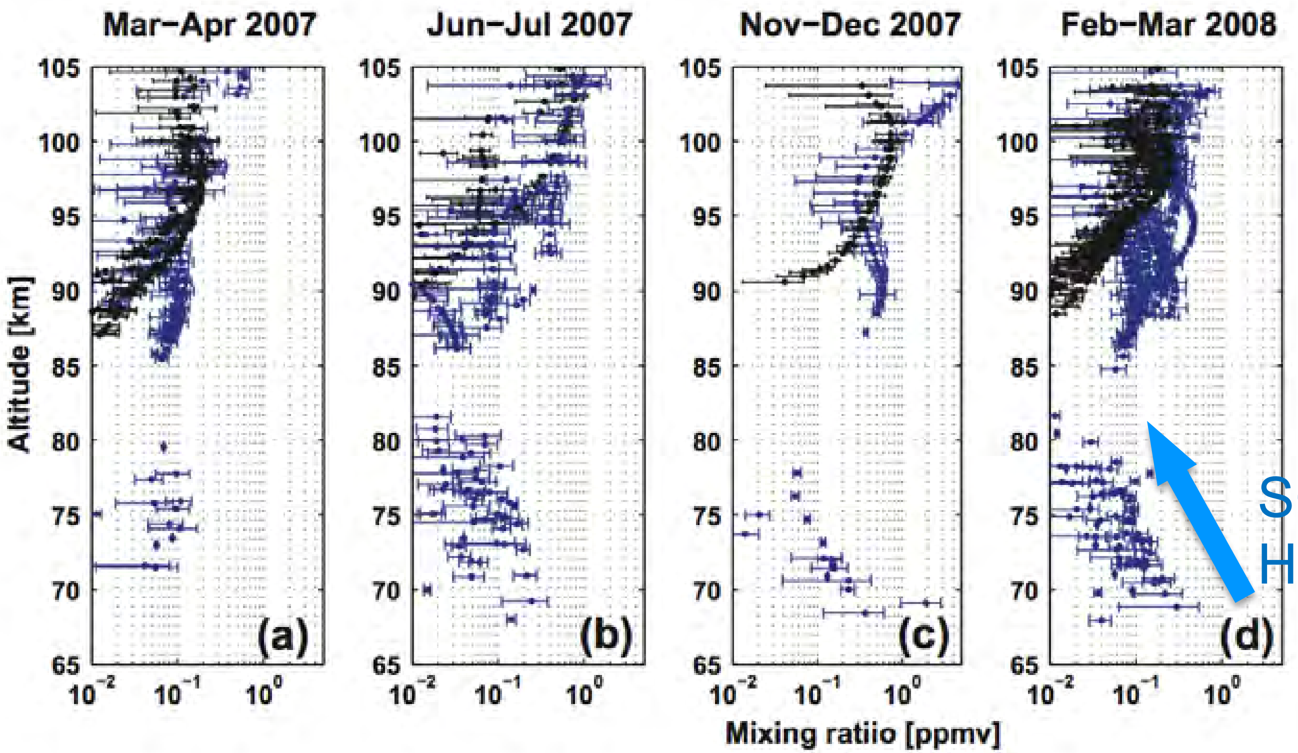

SO_2 loss through H_2SO_4 production

Enhancement at high altitudes cannot be explained by existing photochemical models.

Solar occultation by Venus Express/SPICAV-SOIR

Venus’ haze layer above clouds

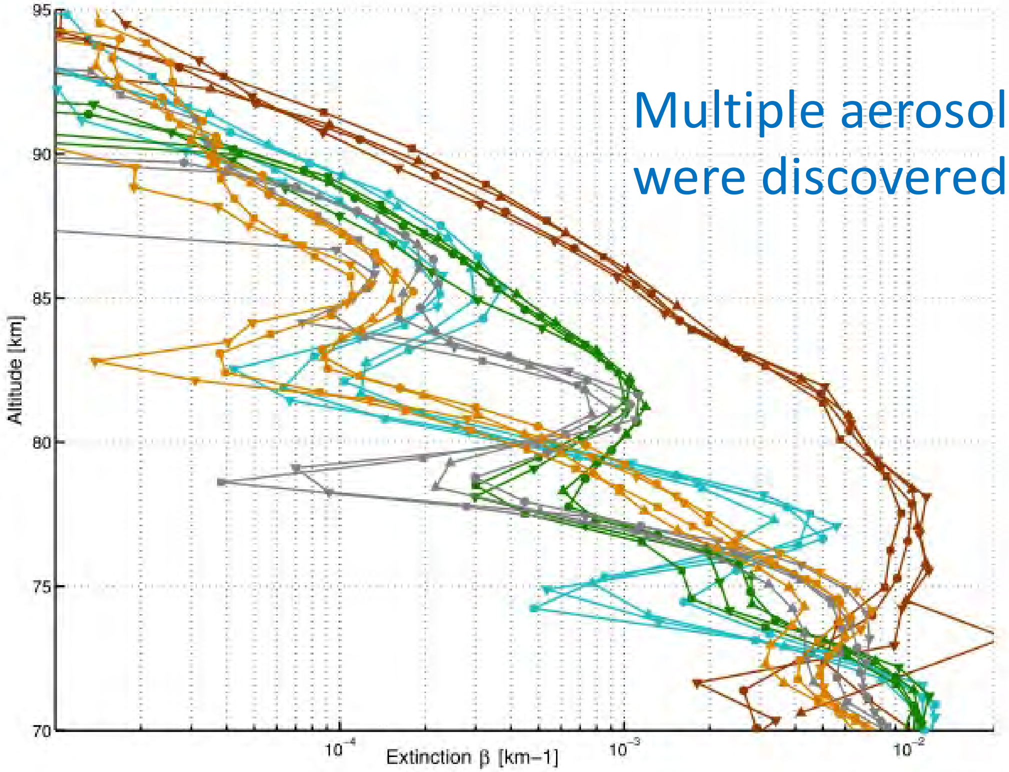

Multiple aerosol layers were discovered

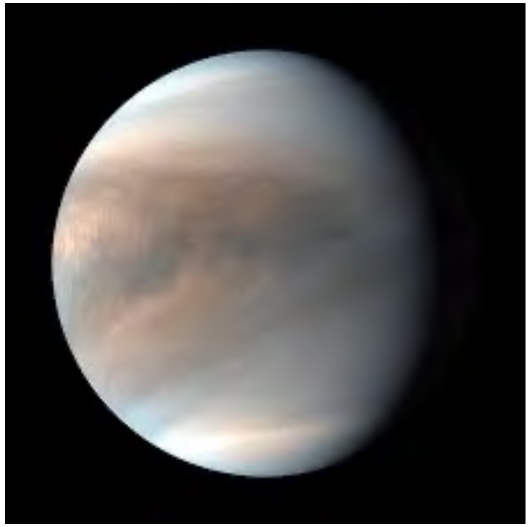

Wilquet et al. (2009)

Stellar occultation by Venus Express/SPICAV

Stellar occultation can cover all local times

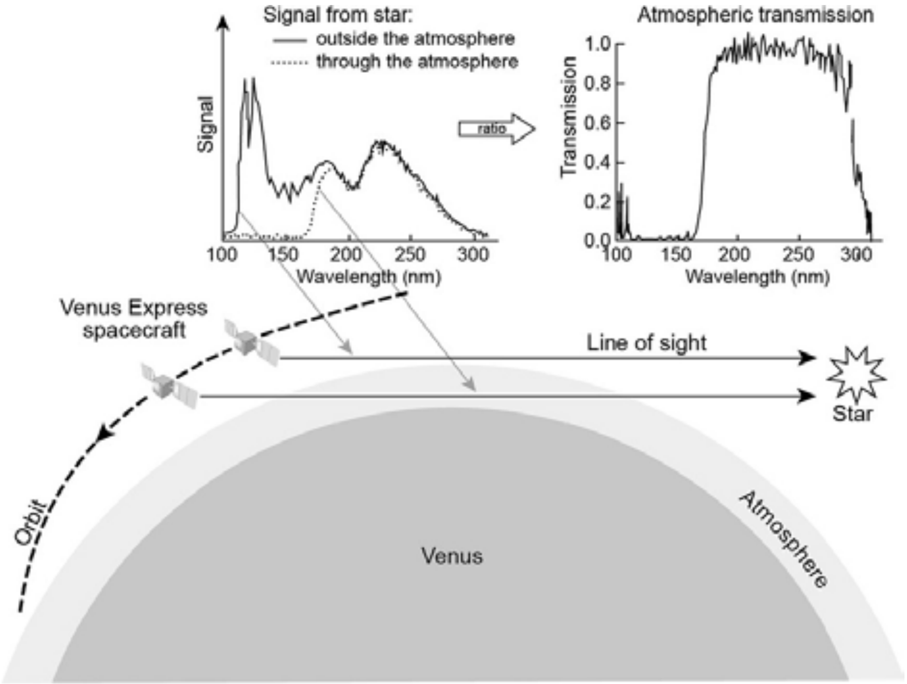

Taylor et al. (2018)

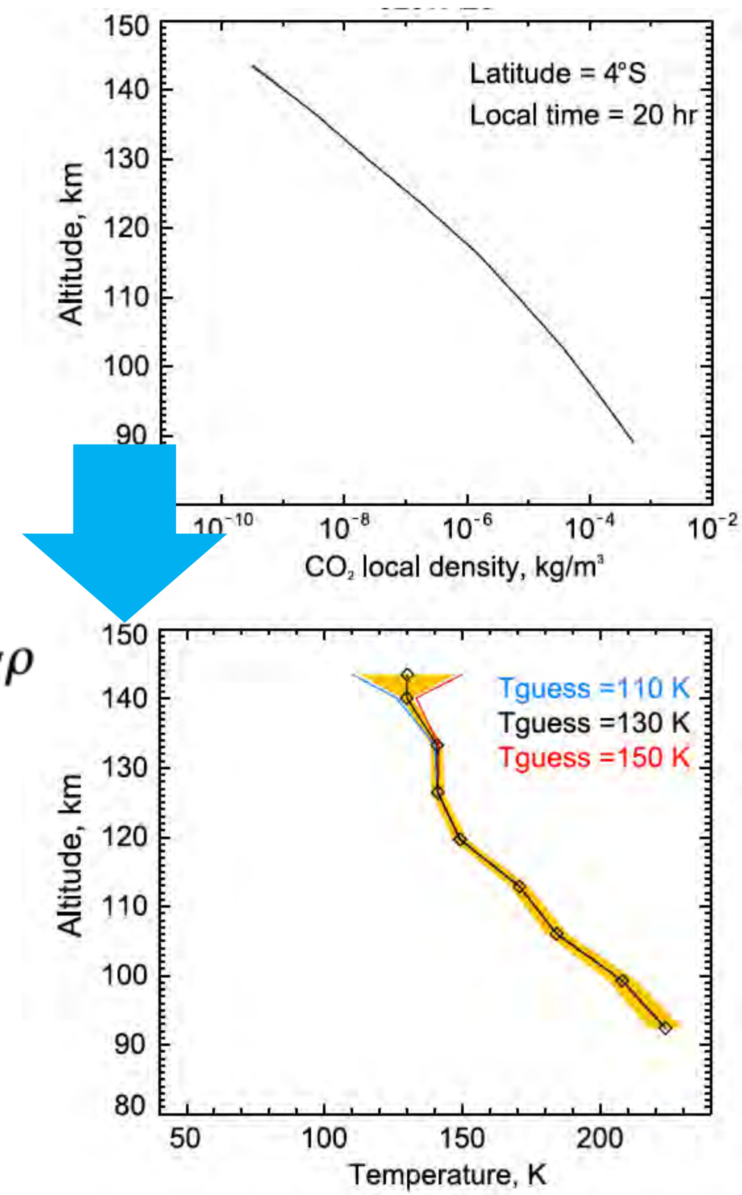

$$\frac{dp}{dz} = -g\rho$$

Piccialli et al. (2015)

Nadir infrared sounding:

- can cover all local times
- sensitive to temperature

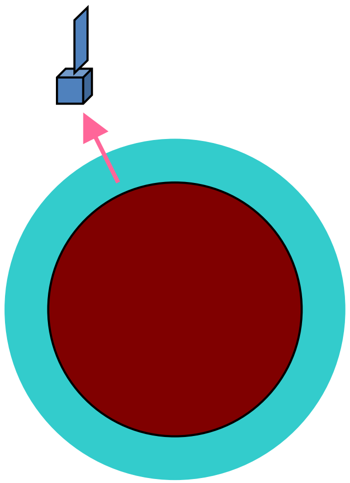

Thermal emission spectra of Mars measured by Mariner 9/IRIS

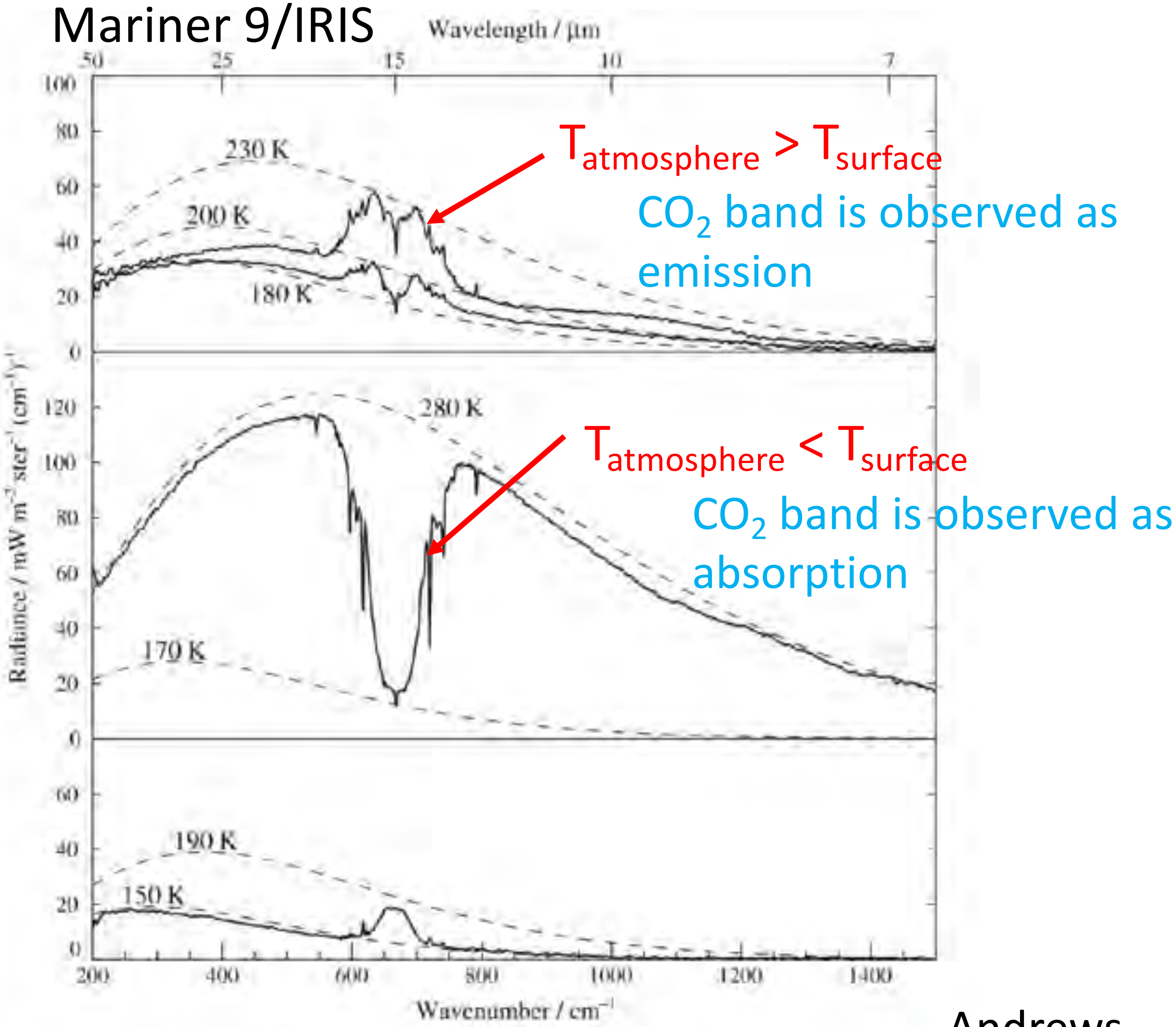

Emission spectra from Mars obtained with the IRIS instrument on Mariner 9 (adapted from Hanel *et al.* (1972)). Top panel: spectra recorded over the south polar region; upper curve includes a smaller fraction of the polar ice cap than the lower curve. Middle panel: spectrum recorded near 21° S. Lower panel: spectrum recorded near 66° N; note that the condensation temperature of CO_2 at Martian surface pressures is about 145 K. Diagram prepared with the help of Dr S. R. Lewis, using data from the Planetary Data System.

Andrews (2010)

Martian water vapor: Mars Express PFS/LW observations of thermal infrared emission (Fouchet et al. 2007)

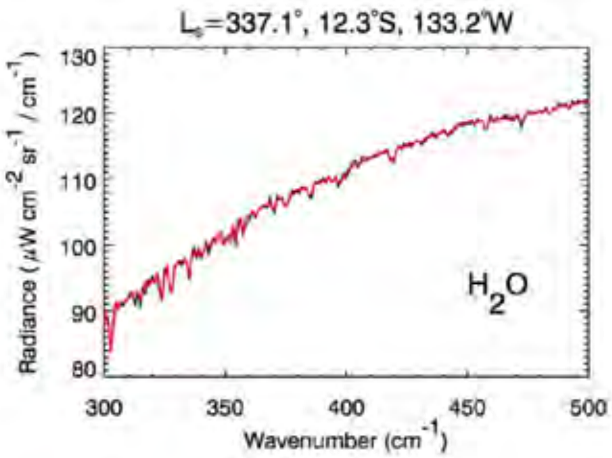

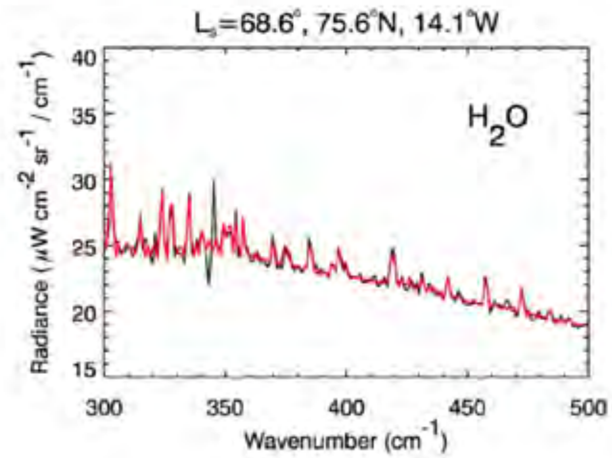

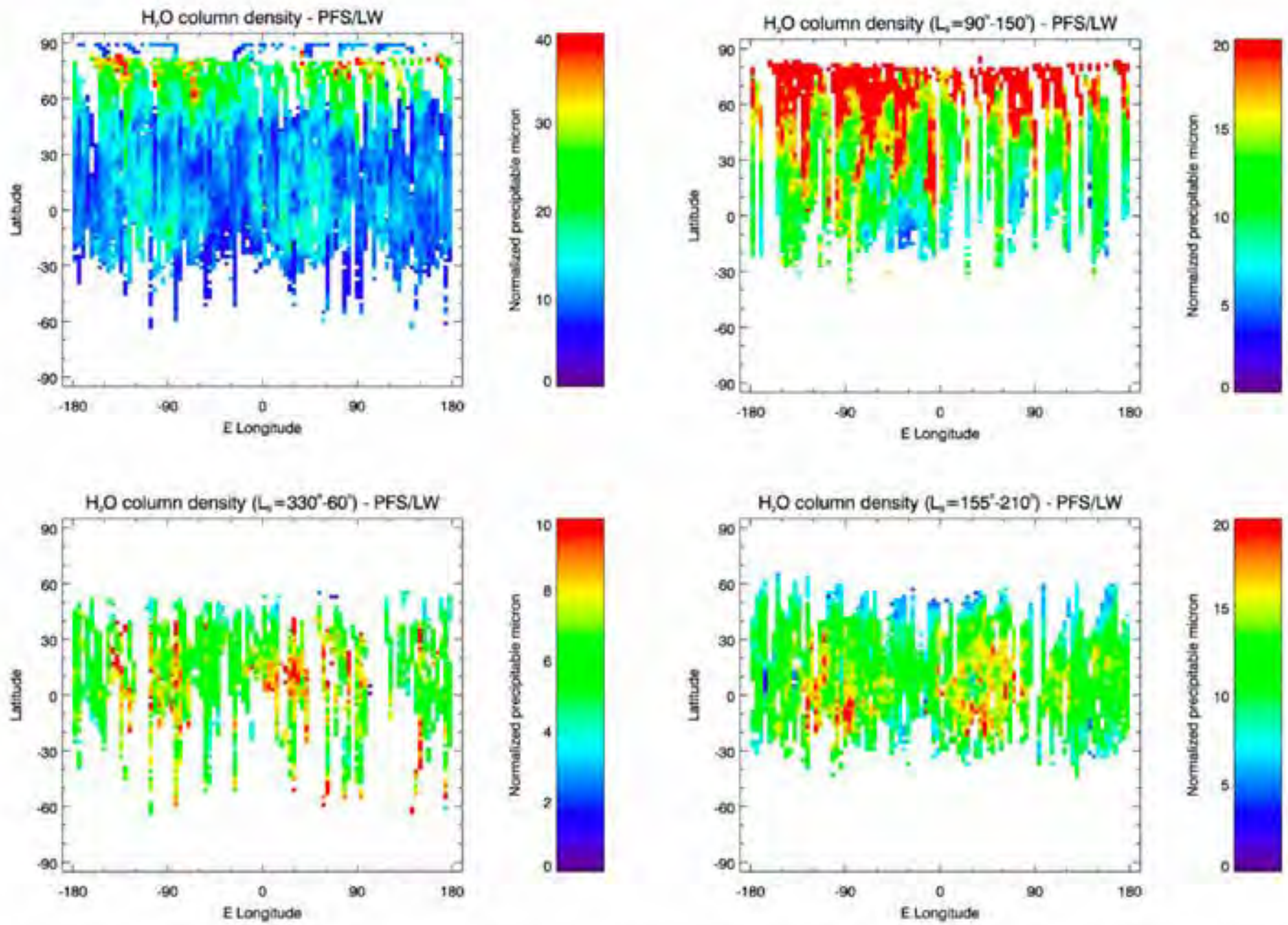

Fig. 6. Geographical distribution of water. Water columns are here normalized to a common 610 Pa pressure. Top left: entire dataset. Top right: $L_s = 330°–60°$. Bottom left: $L_s = 90°–150°$. Bottom right: $L_s = 155°–210°$.

Retrieval of vertical structures from nadir-looking thermal infrared spectra

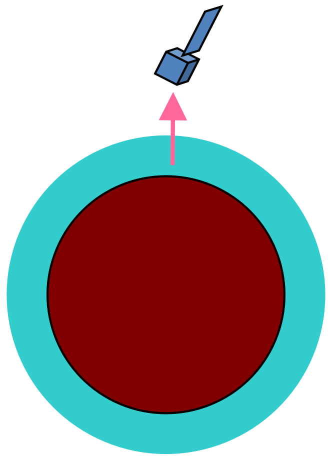

Contribution functions for wavelengths in CO_2 15 µm band for Mars atmosphere

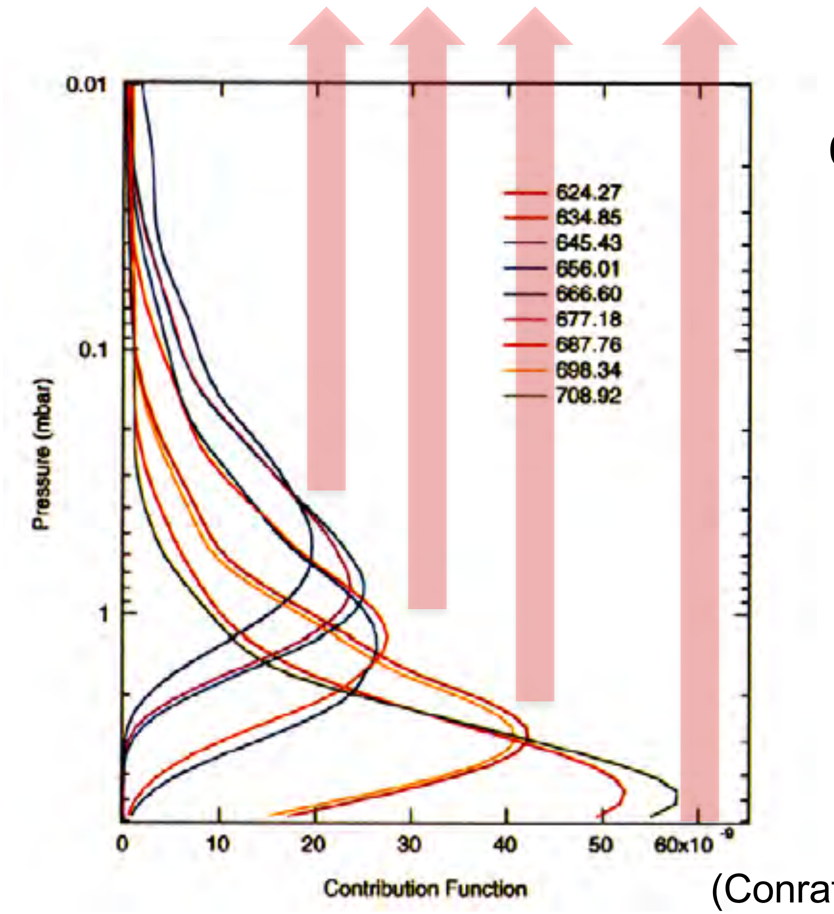

(Conrath et al. 2000)

Outgoing radiation:

$$I = \underbrace{B(T_s)\exp(-\tau_s)}_{\text{From surface}} + \underbrace{\int_0^\infty B(T(z))\overset{\text{Contribution function}}{\boxed{k_a(z)\exp(-\tau(z))}}\,dz}_{\text{From atmosphere}}$$

$$\tau = \int_z^\infty k_a\,dz$$: optical depth

I : radiance(J/m2/s/str/Hz)
B : Planck function
τ : optical thickness
k_a : absorption coefficient
z : altitude

Temperature retrieval from infrared spectra taken by Mars Global Surveyor/TES

temperature

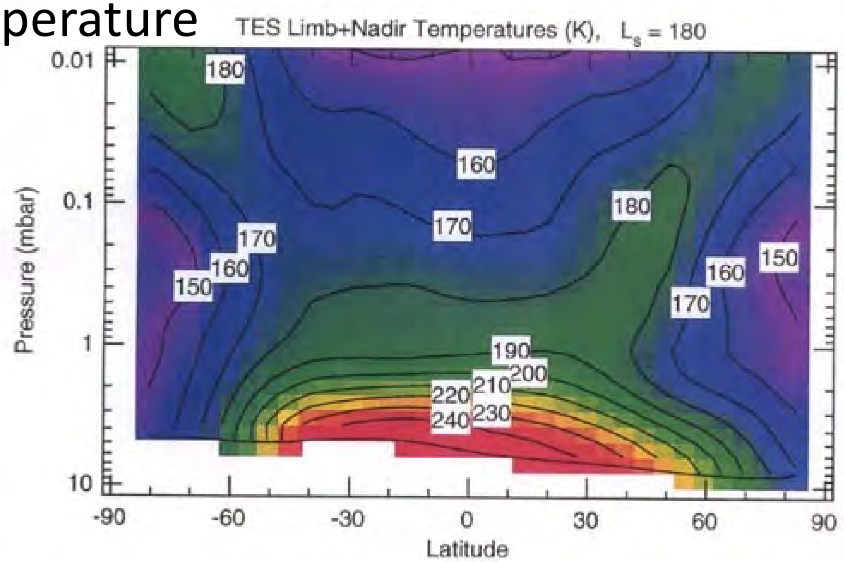

eastward wind

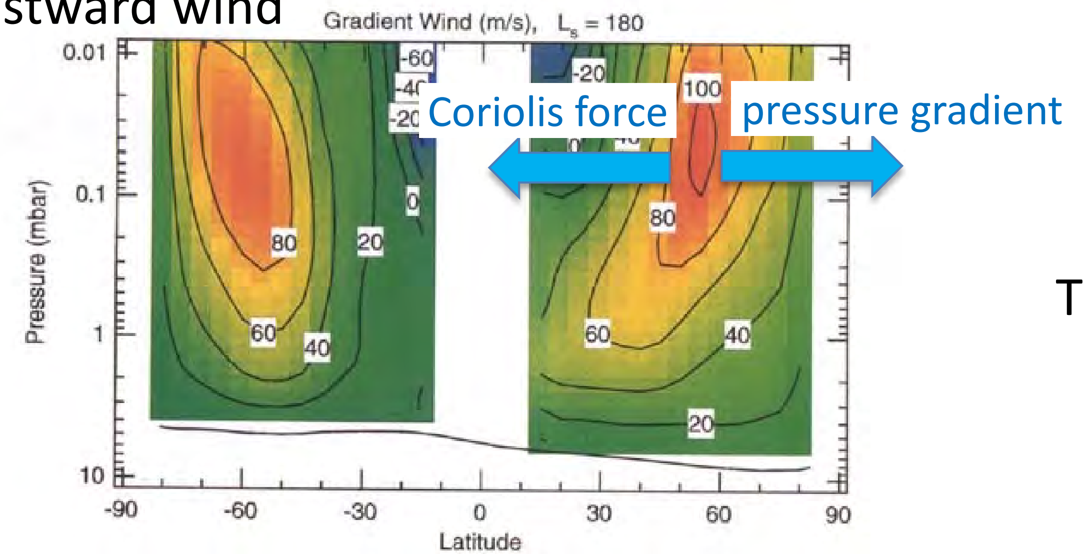

Thermal wind : $$\frac{\partial u_g}{\partial p} = \frac{R}{fp}\frac{\partial T}{\partial y}$$

Smith et al. (2001)

Contribution functions for Venus atmosphere

（Schofield & Taylor 1983）

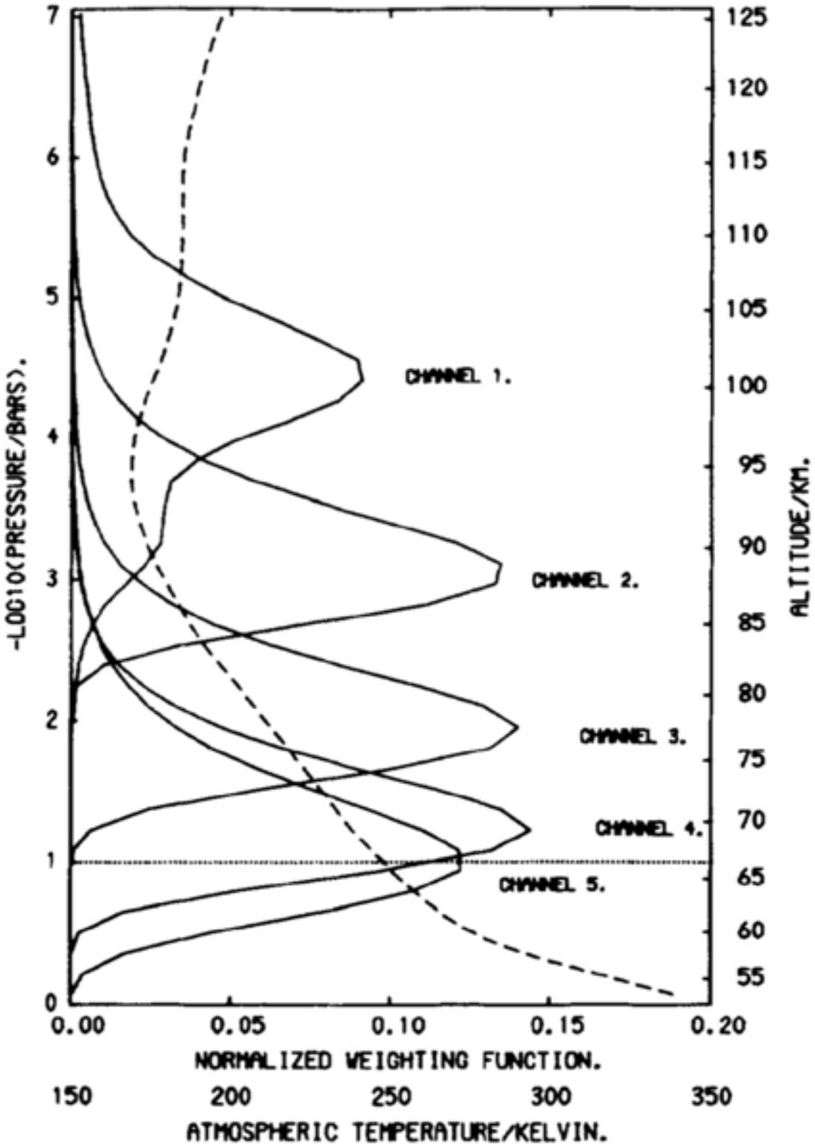

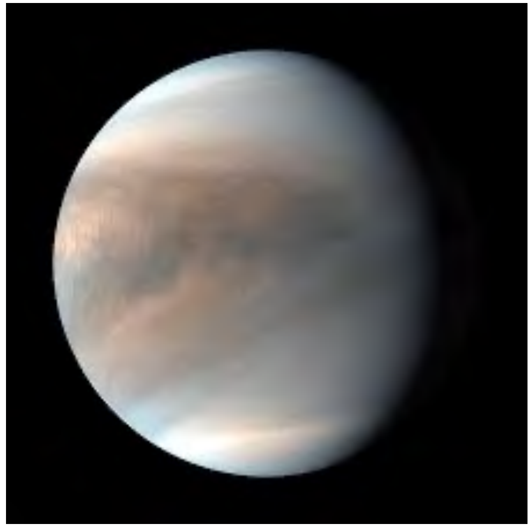

TABLE 1. OIR TEMPERATURE-SOUNDING CHANNELS – OPTICAL PROPERTIES

Channel*	Field of view** full angle (degrees)	Effective wavelength† (cm^{-1})	Effective wavelength† (μm)	Spectral resolution†† (cm^{-1})
1	5·0	667·0	15·0	0·005
2	1·25	679·4	14·7	10·7
3	1·25	727·2	13·8	12·0
4	1·25	764·4	13·1	14·3
5	1·25	872·0	11·5	22·3

Retrieved temperature distribution of Venus atmosphere (Schofield & Taylor 1983)

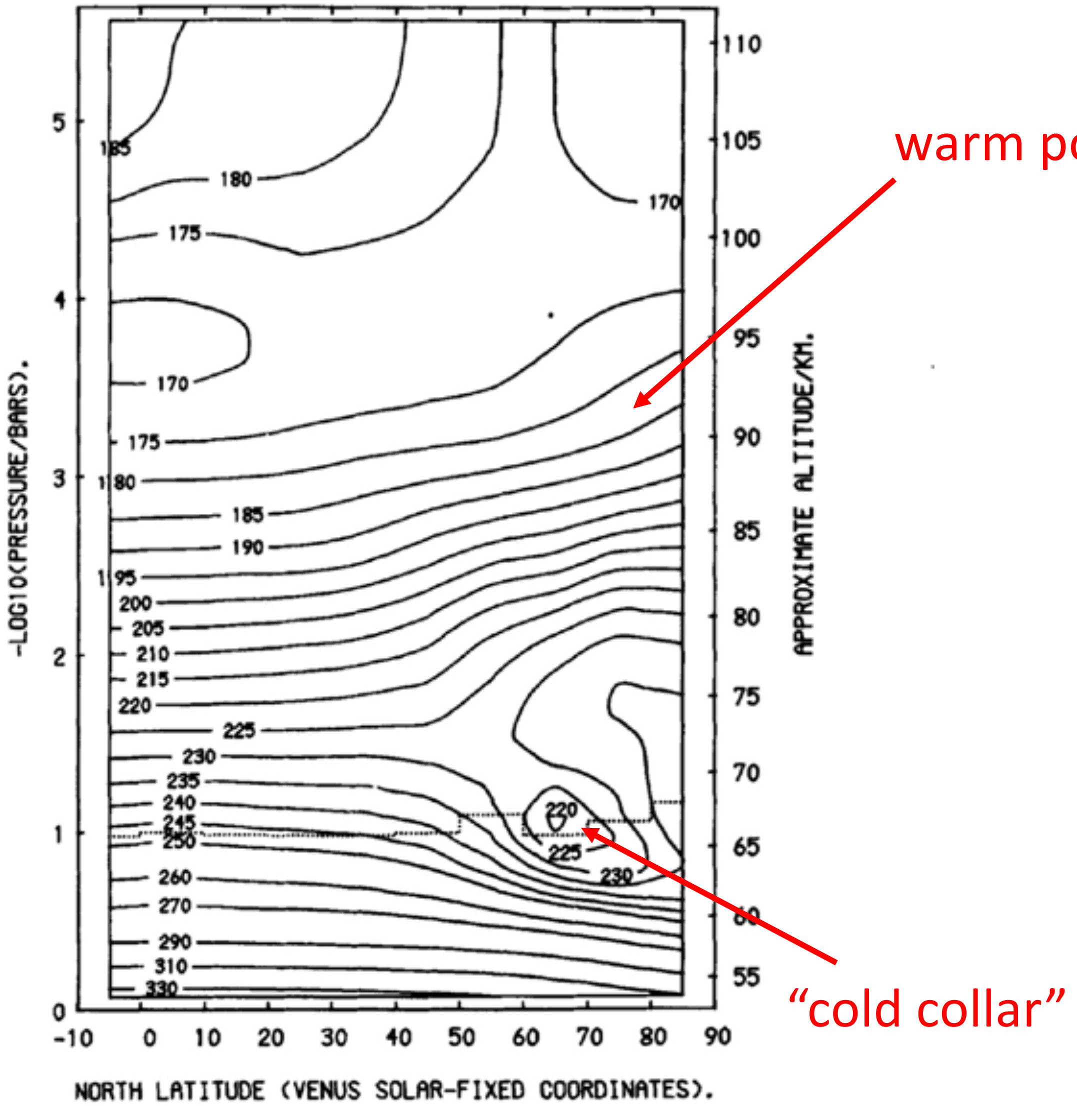

Figure 9. The retrieved zonal-mean temperature field and cloud structure. The temperature field is contoured as a function of pressure and latitude, and the altitude scale is averaged over latitude. Cloud unit optical depth at 11·5 μm is indicated by a dotted line.

Thermal infrared images of Venus cloud obtained by Akatsuki LIR

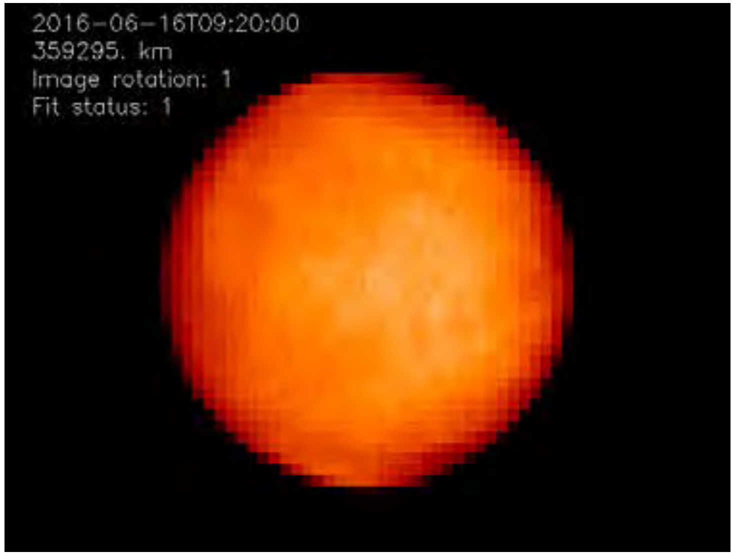

Near-infrared windows of Venus

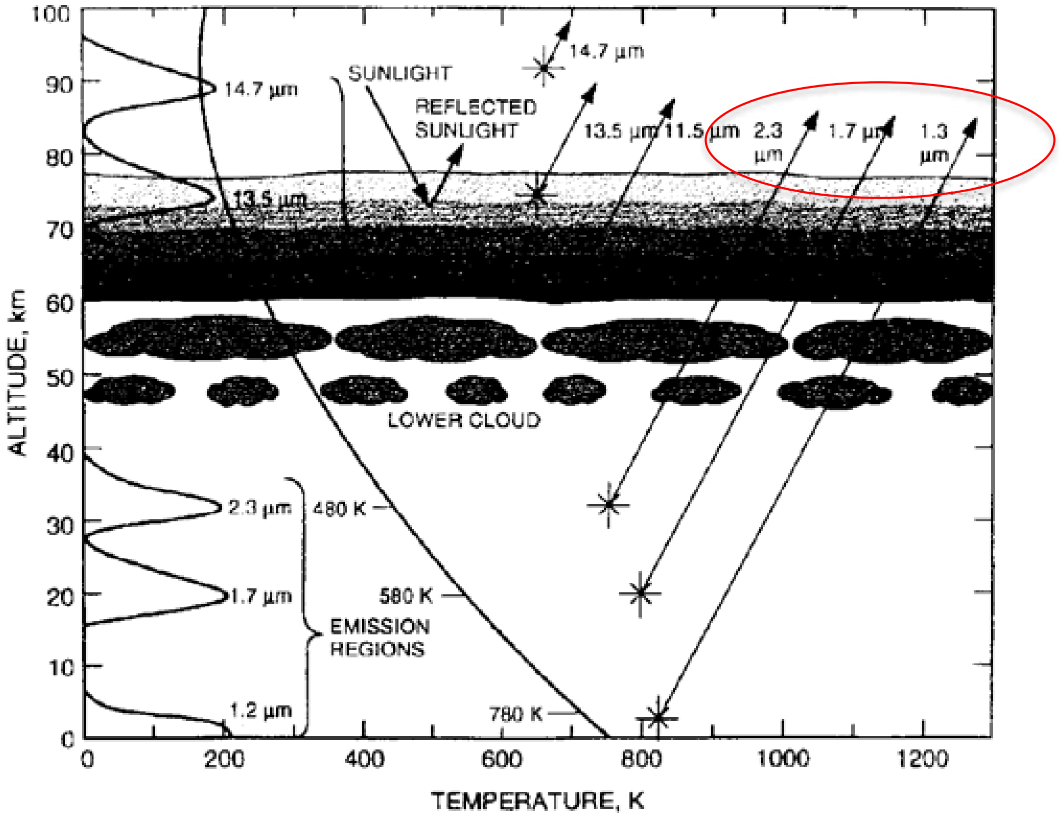

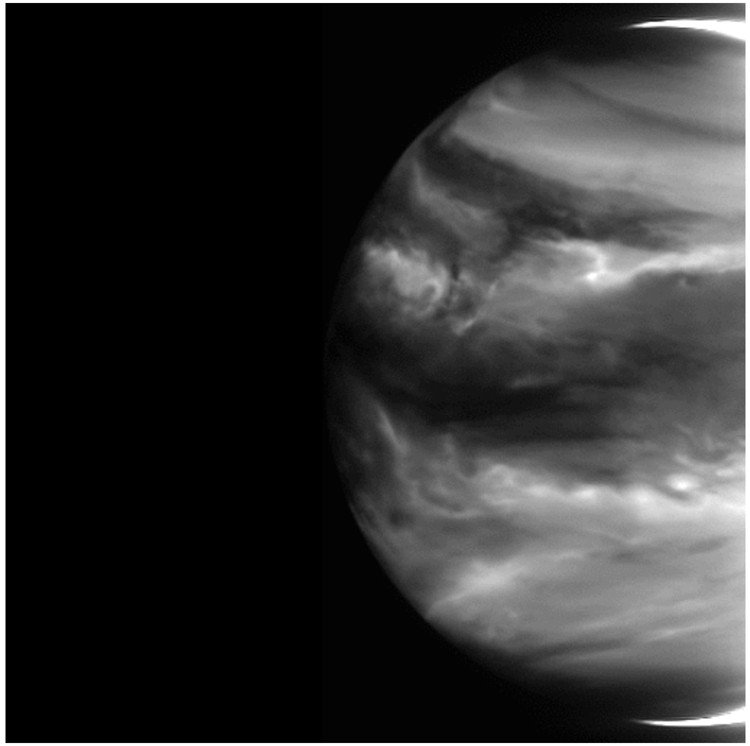

2.26-µm images taken by Akatsuki/IR2

Retrieval of the atmospheric composition of Venus from infrared spectra taken by ground-based telescopes

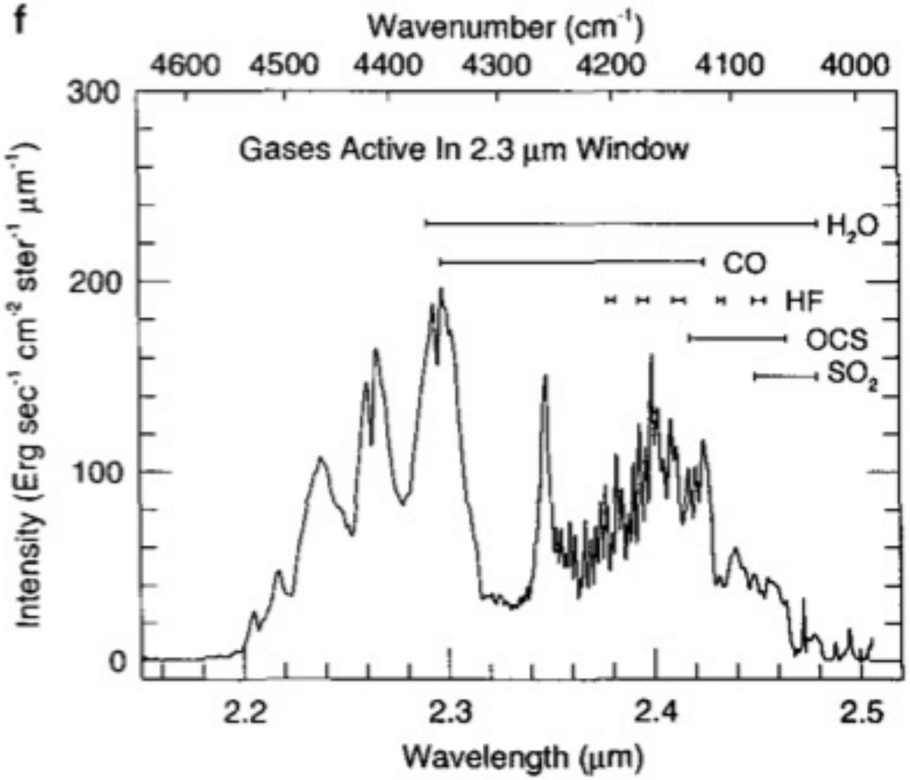

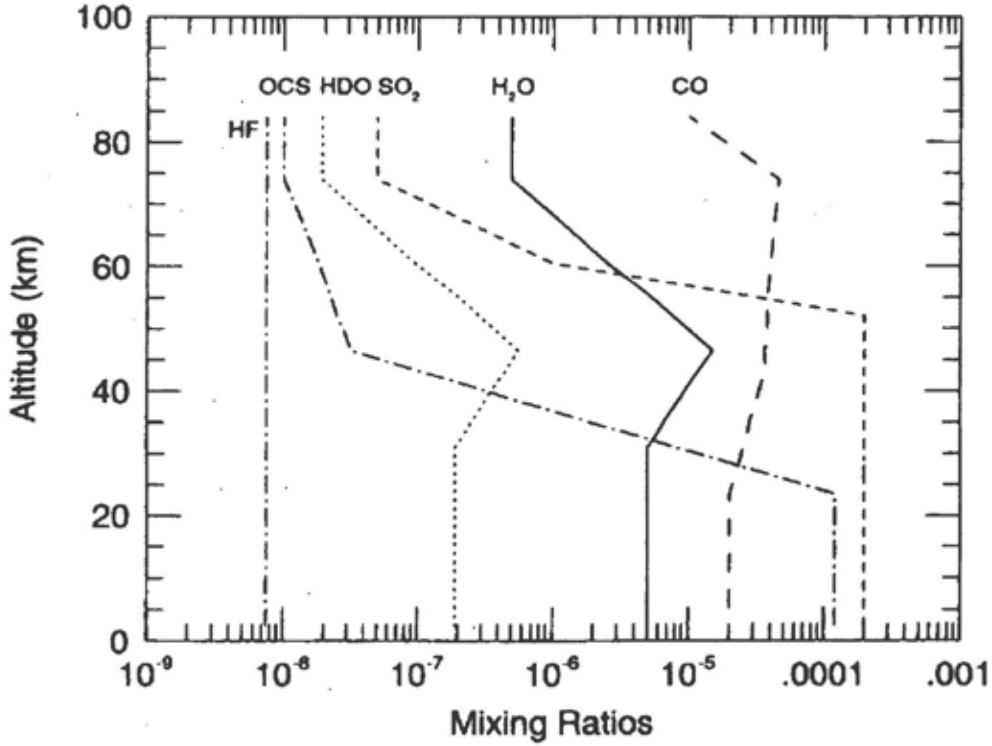

Pollack et al (1993)

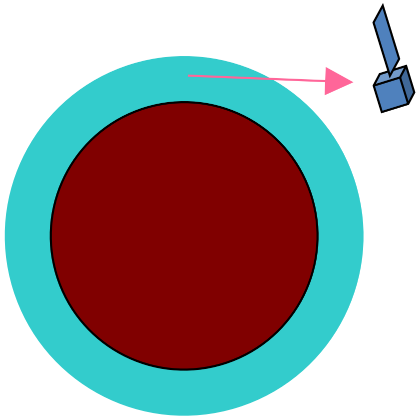

Spectroscopy of limb thermal emission

Doppler wind measurements of the Venusian thermosphere
from sub-millimeter CO absorption line observations
Clancy et al. (2012)

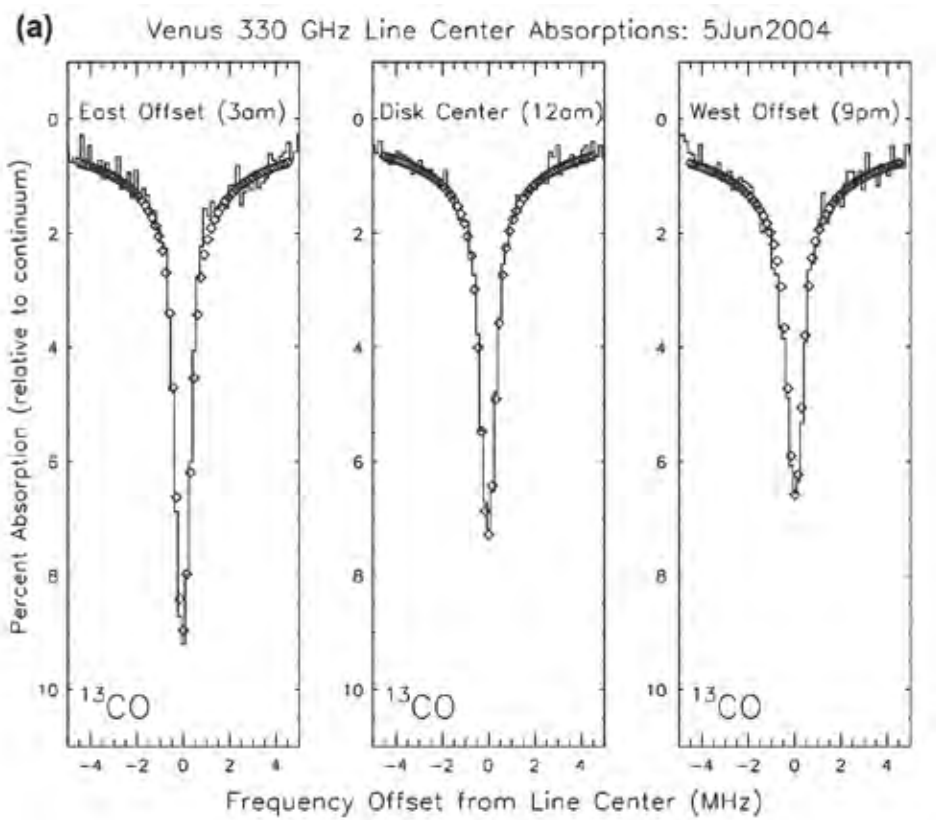

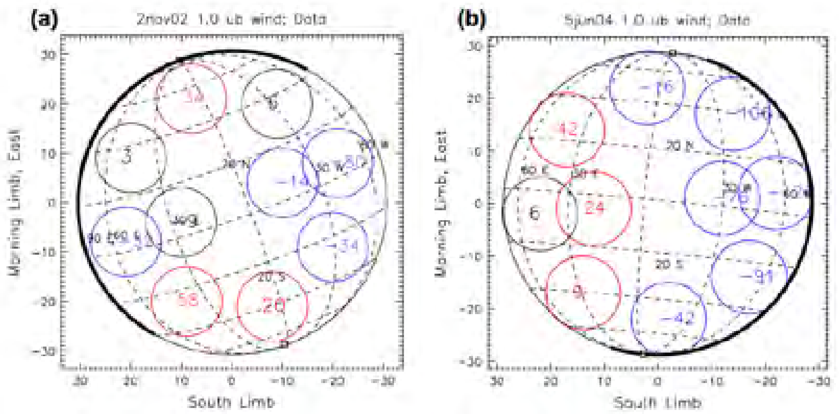

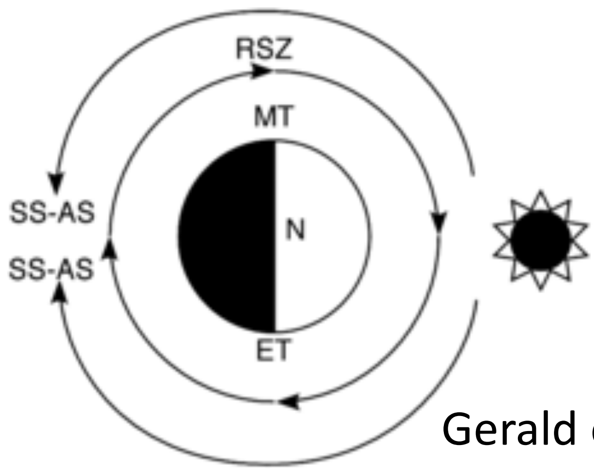

Gerald et al. (2017)

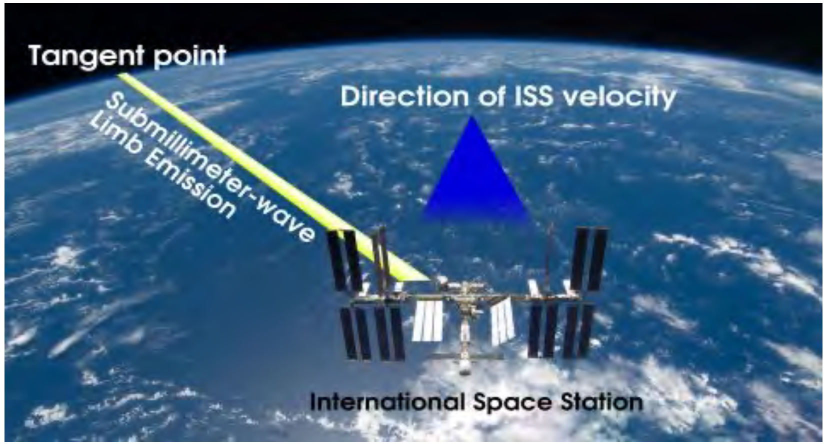

Limb spectroscopy of far-infrared emission from Earth’s stratosphere：ISS/SMILES

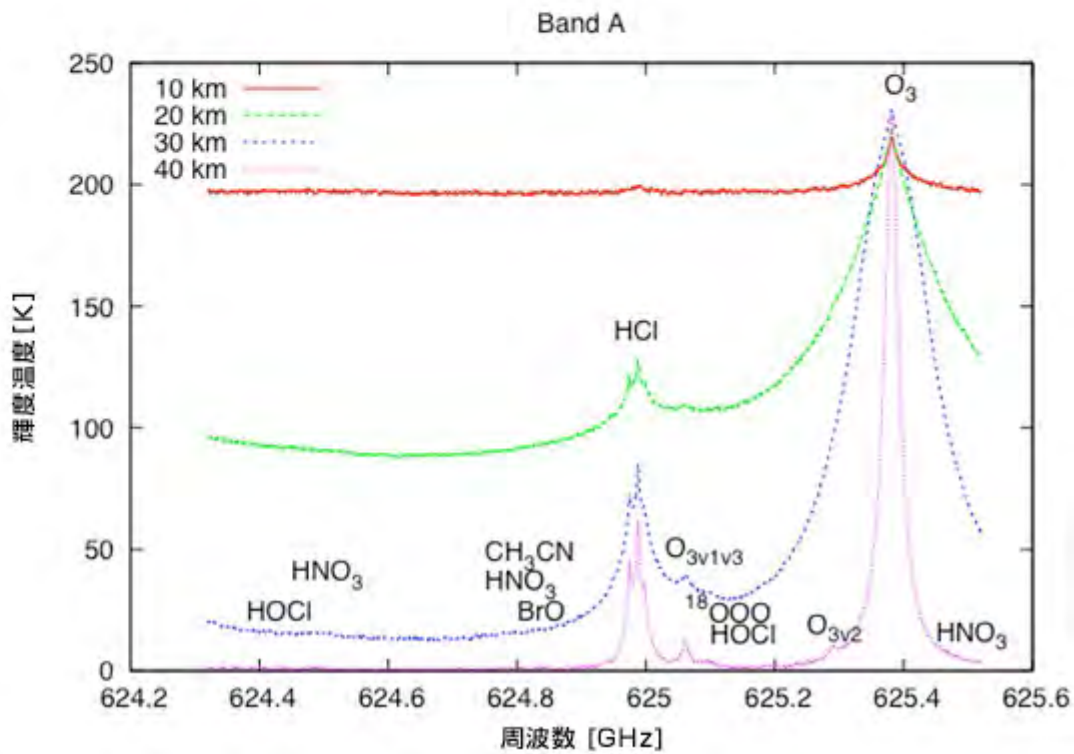

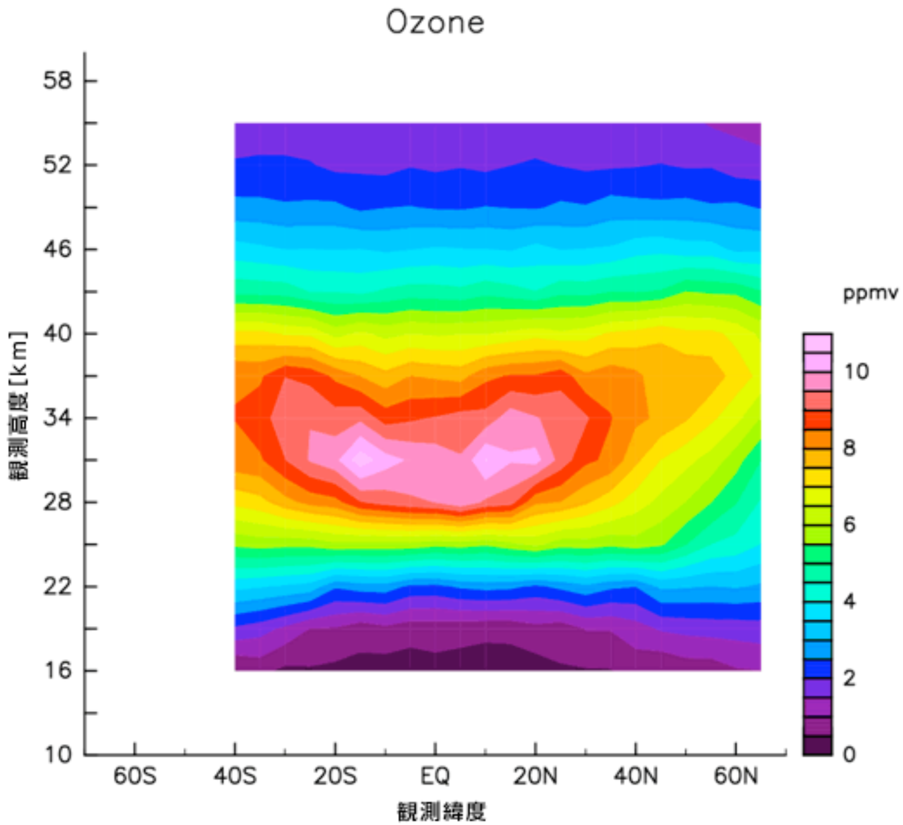

UV backscatter:

sensitive to trace gases
in the upper atmosphere

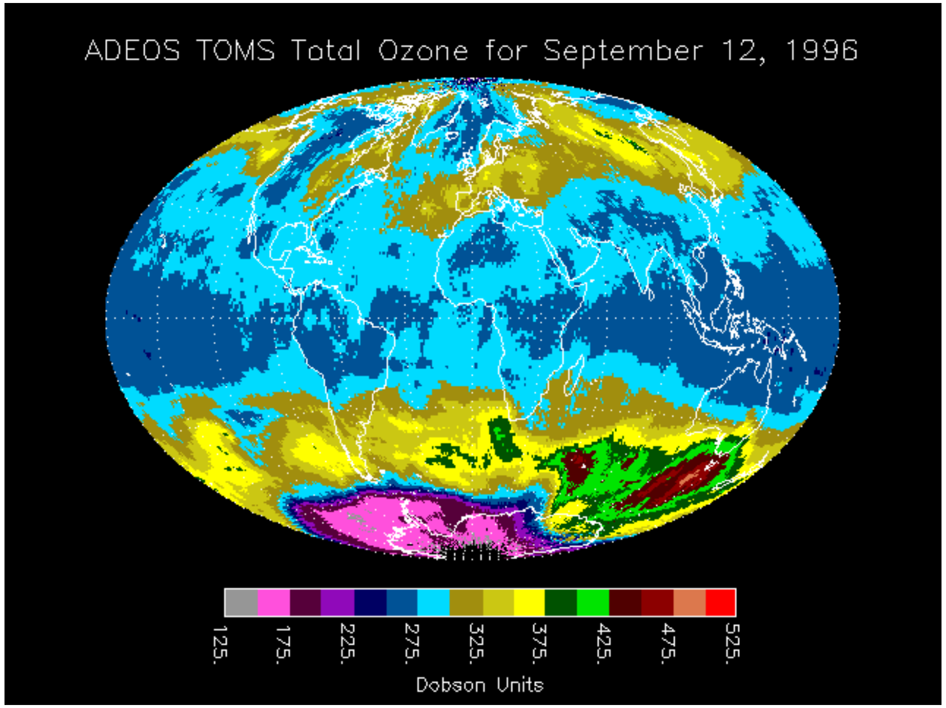

Solar backscatter UV spectroscopy: Total ozone mapping spectrometer (TOMS)

6 bands : 308.6, 312.5, 317.5, 322.3, 331.2, 360.0 nm

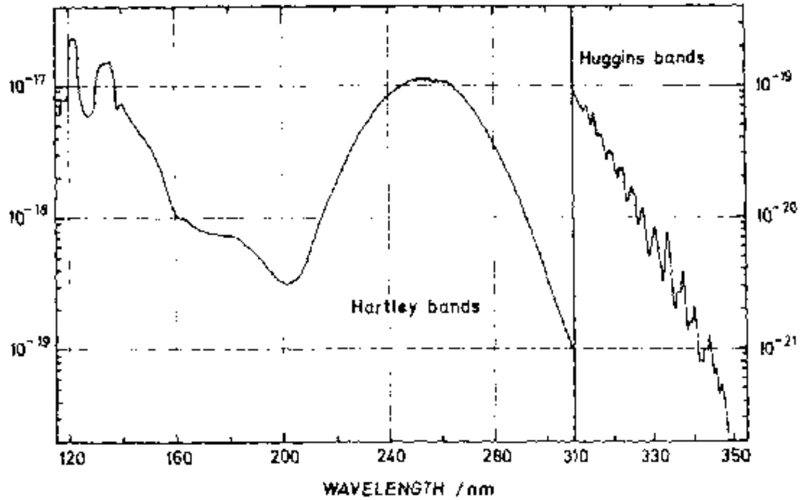

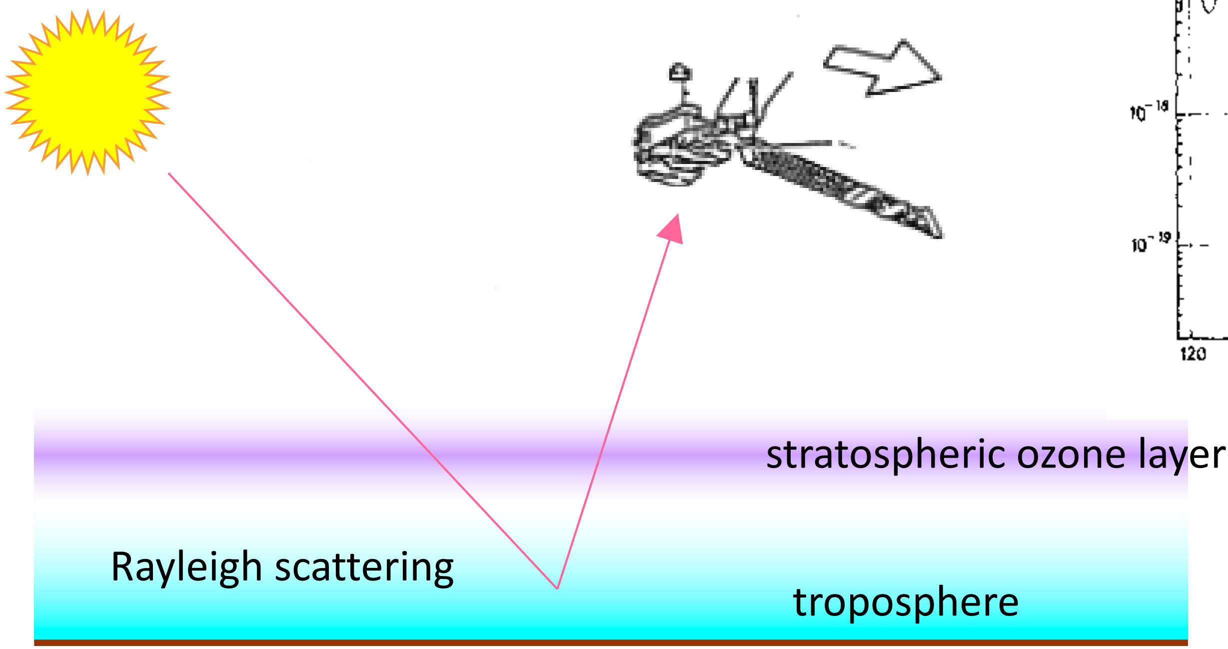

Infrared reflection:

sensitive to trace gases in the lower atmosphere

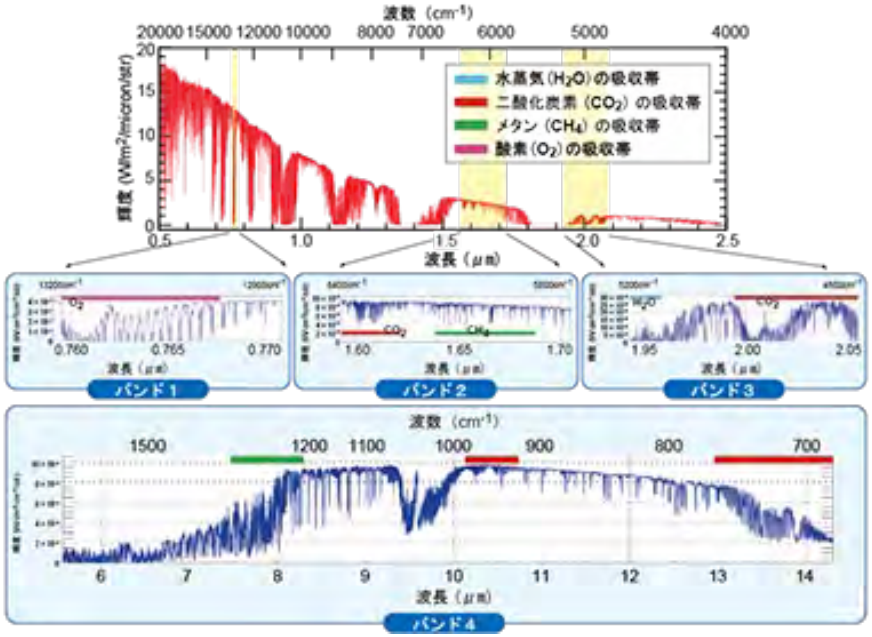

GOSAT

Fourier Transform Spectrometer

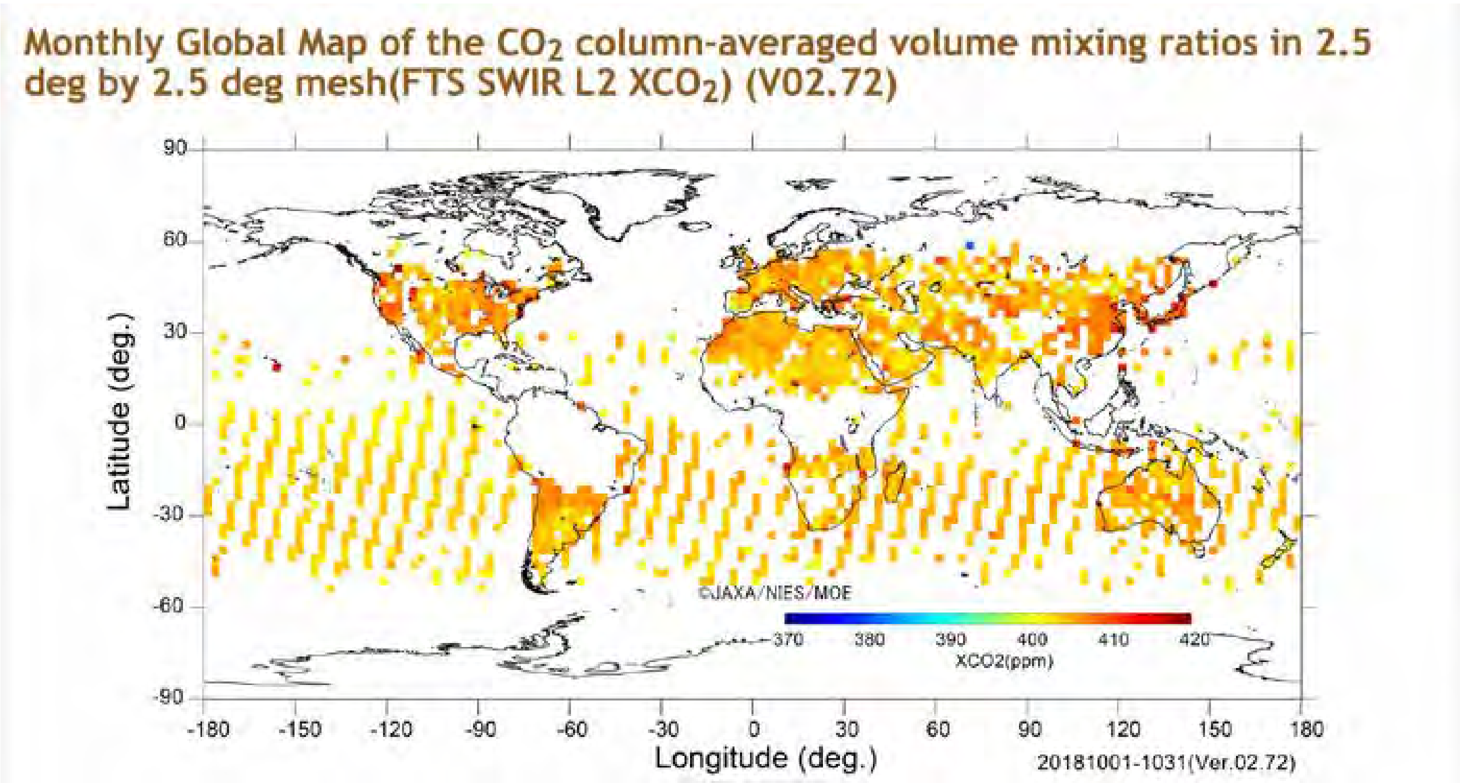

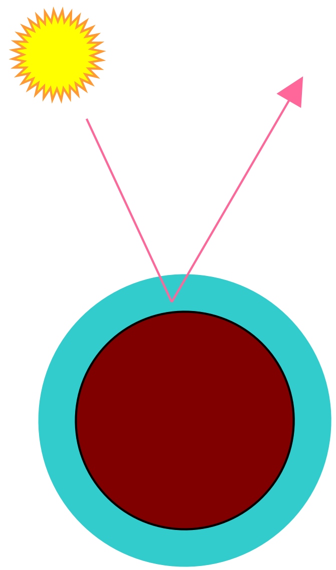

Ground-based observation of methane in Mars atmosphere: utilizing Doppler shift to remove the effect of Earth's methane

Mumma et al. (2009)

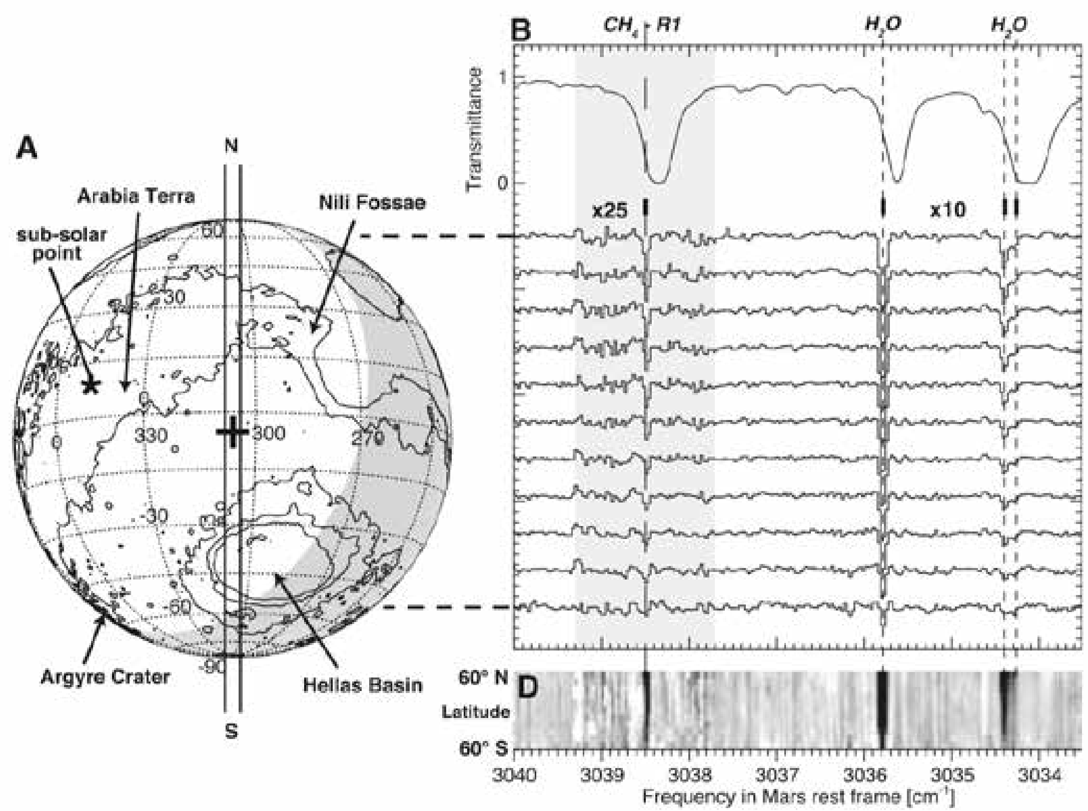

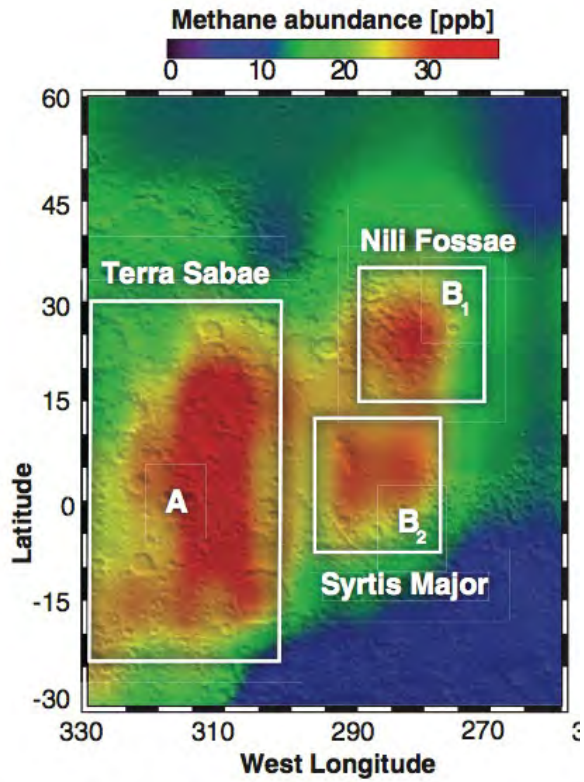

Transit spectroscopy of exoplanets

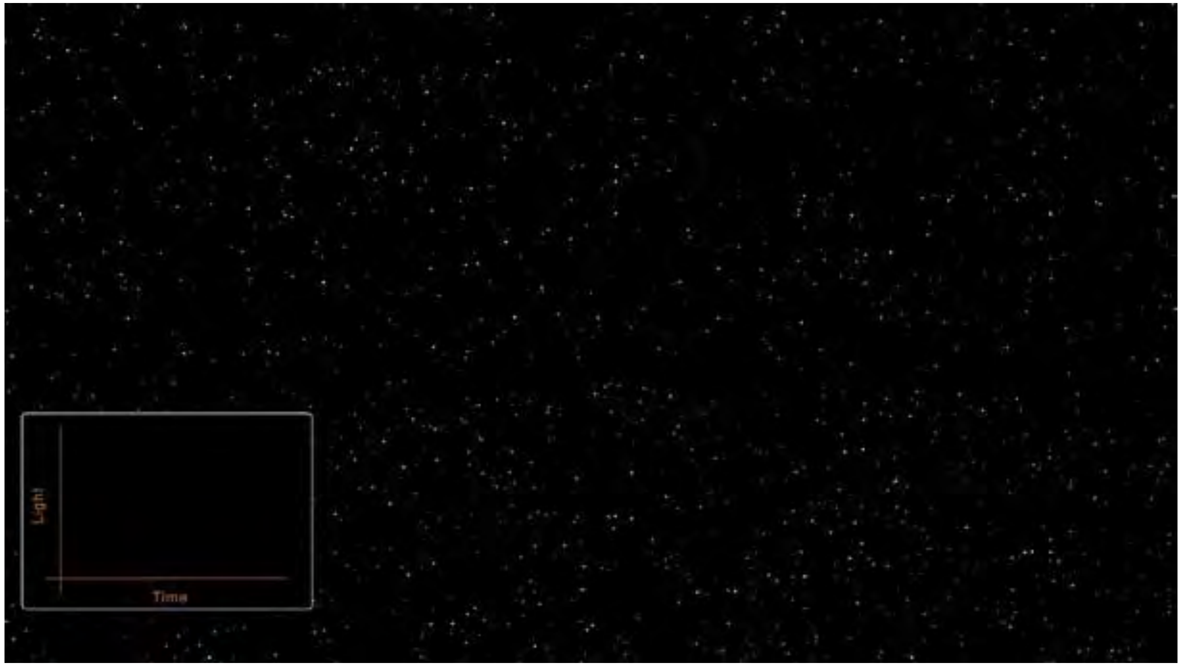

©NASA

"Limb-viewing" spectroscopy of exoplanets

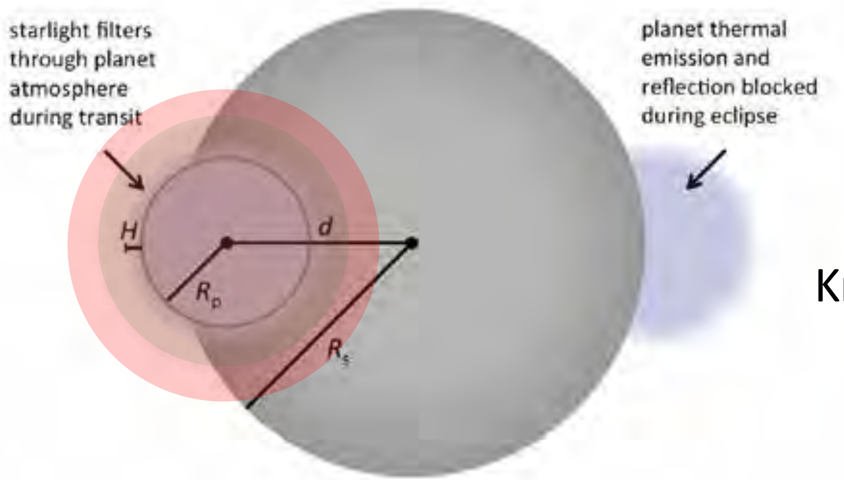

Kreidberg (2018)

Howe & Burrows (2018)

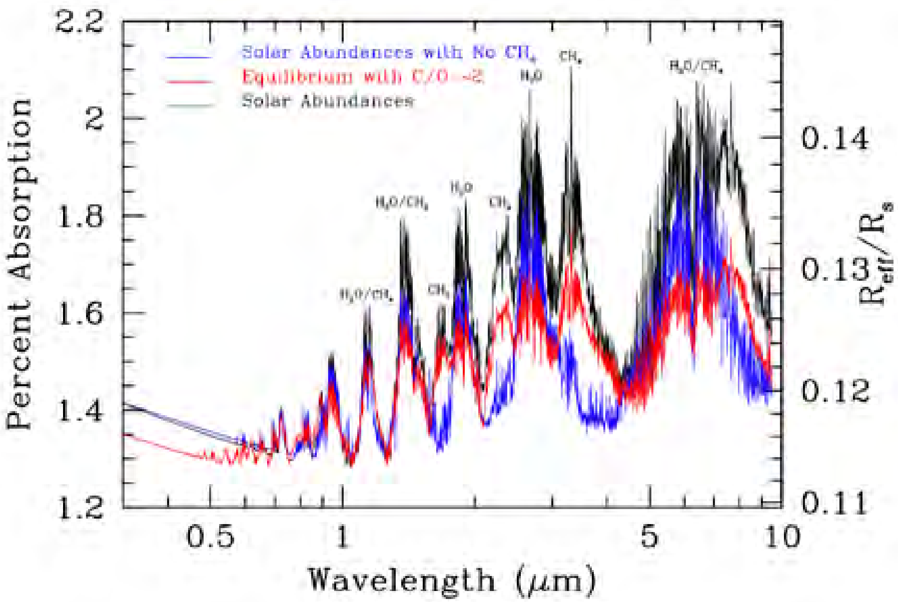

hydrogen-rich atmospheres with non-solar relative abundances

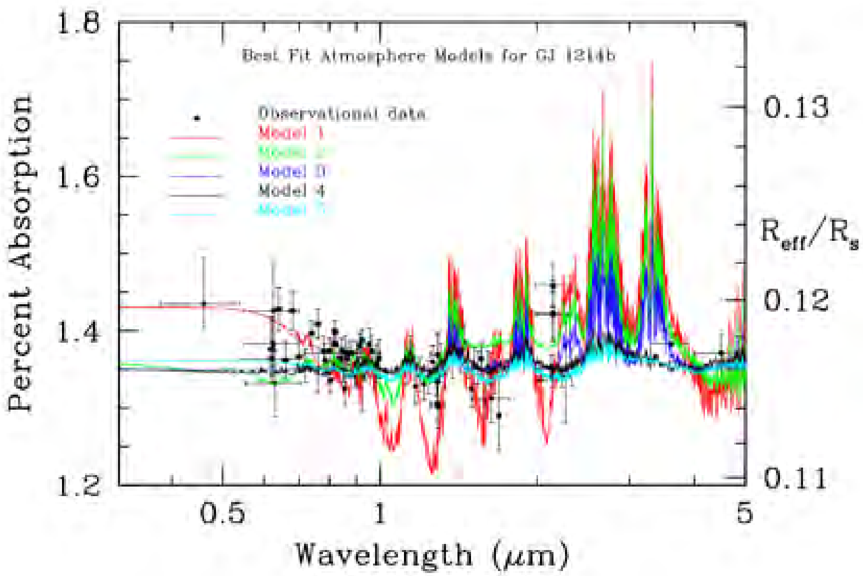

Models 1-3 use a solar-abundance atmosphere, while Models 4 and 5 use an atmosphere of 1% H_2O and 99% N_2

Imaging observation

Himawari (meteorological satellite) imaging channels

JMA Himawari HP

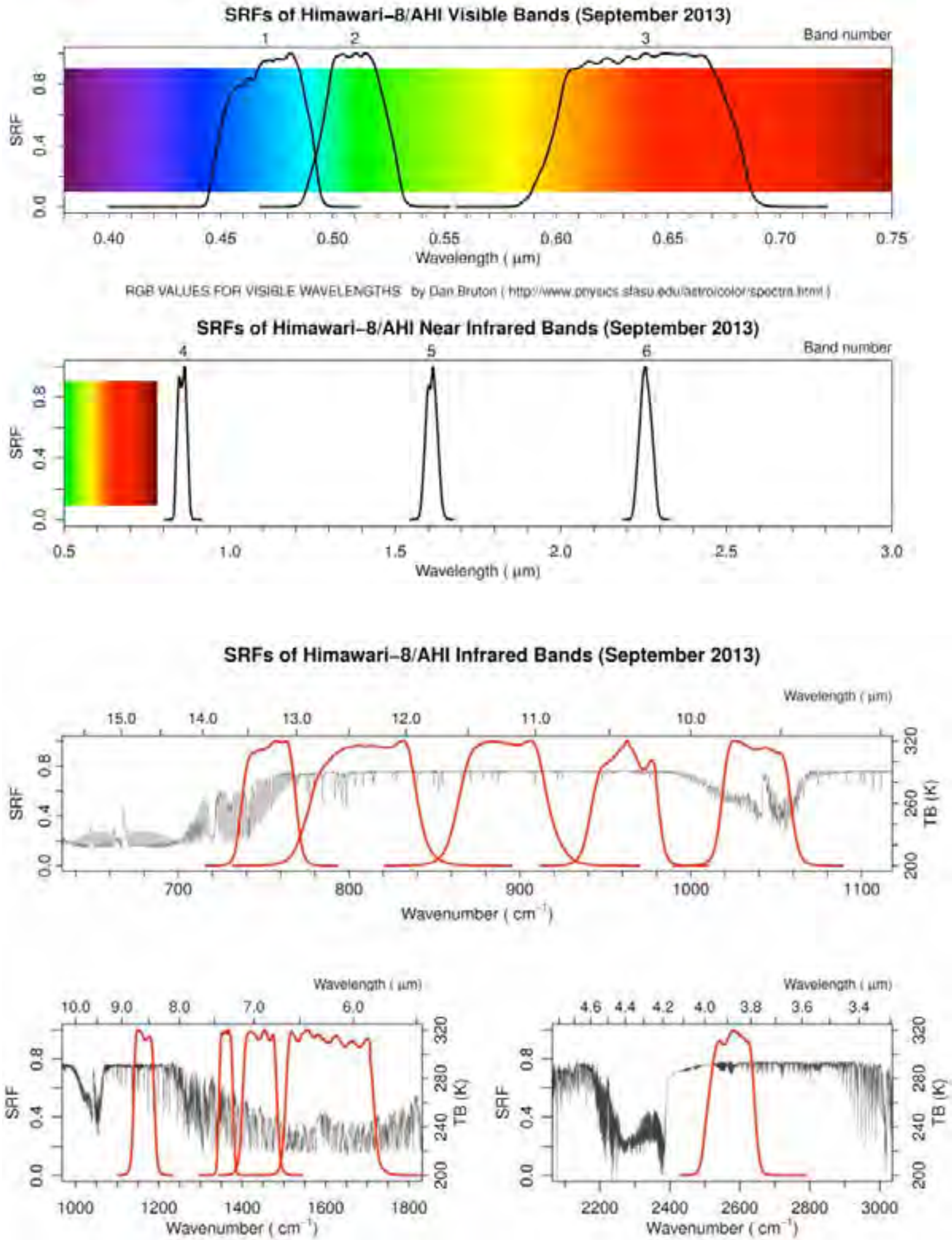

Interference filter

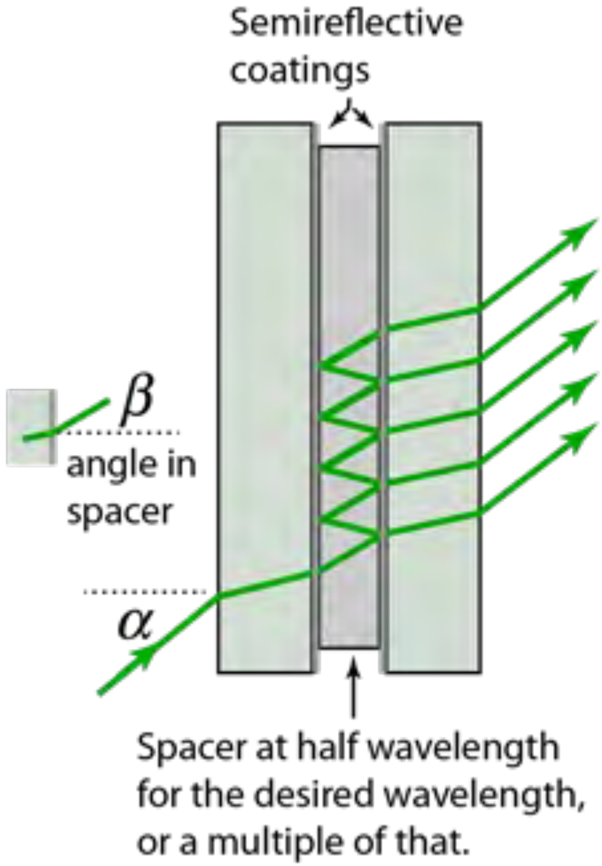

$$d = \frac{\lambda}{2n\cos\beta}$$


visible channel

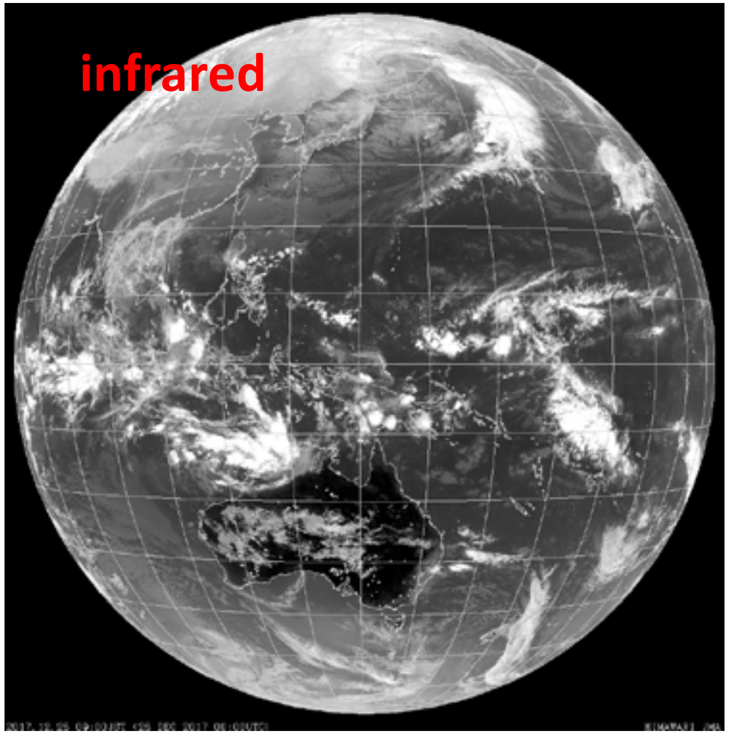
infrared

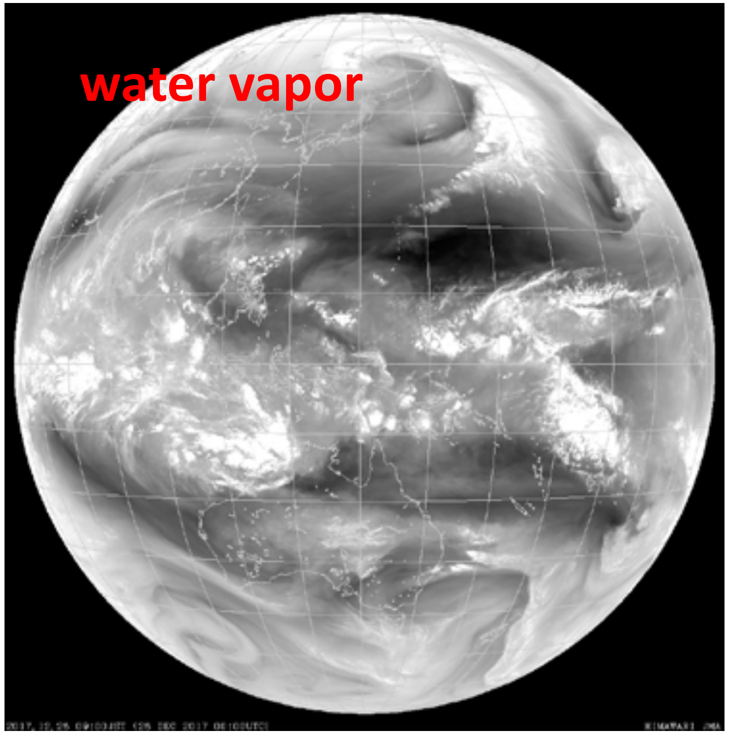
water vapor

Cloud tracking

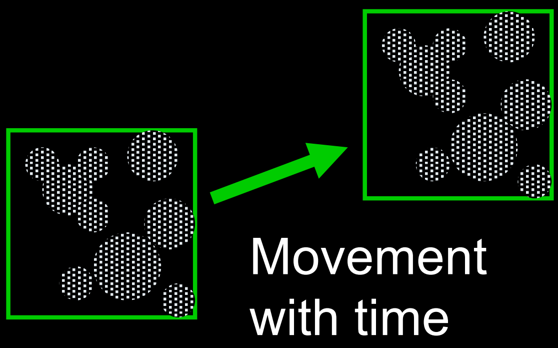

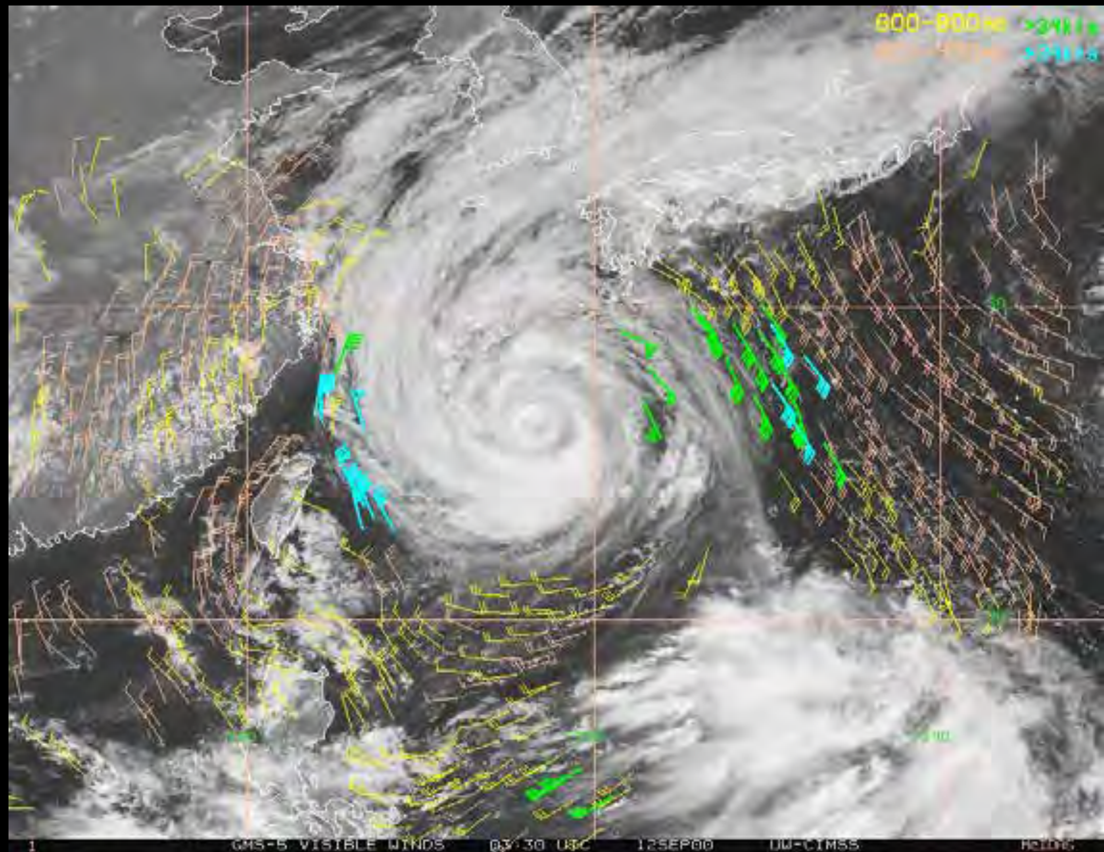

Cloud tracked winds on the Earth

Univ. Wisconsin-Madison/CIMSS HP

Venus orbiter AKATSUKI

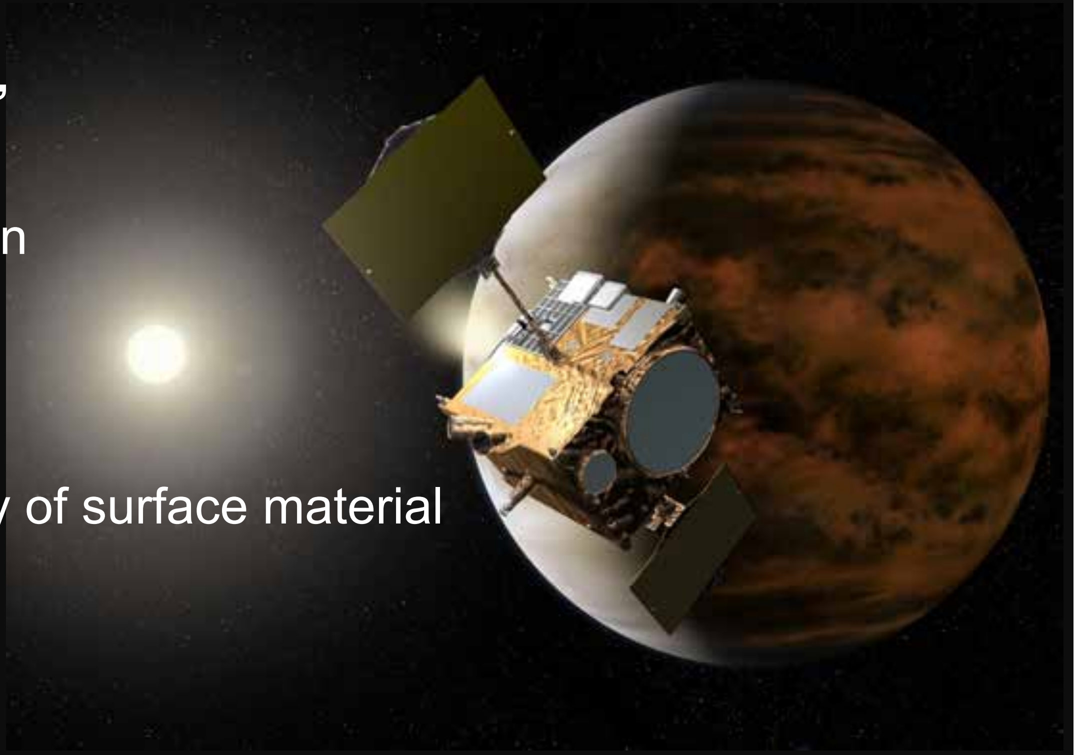

- Science target : **'Weather of Venus'**
  - Mechanism of 'super-rotation'
  - Structure of meridional circulation
  - Meso-scale processes
  - Formation of clouds
  - Lightning
  - Active volcanism, inhomogeneity of surface material
- Science instruments
  - 1μm Camera (IR1)
  - 2μm Camera (IR2)
  - Longwave IR Camera (LIR)
  - Ultraviolet Imager (UVI)
  - Lightning and Airglow Camera (LAC)
  - Ultra-stable oscillator (USO)
- Launch: May 2010   Arrival: Dec 2015

On-board instruments

five cameras + ultra-stable oscillator

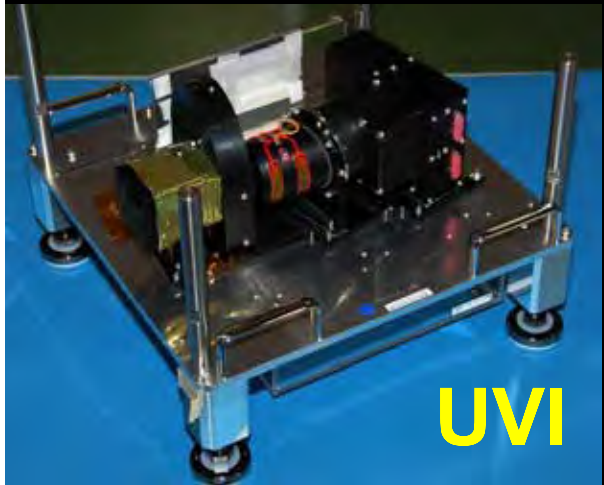

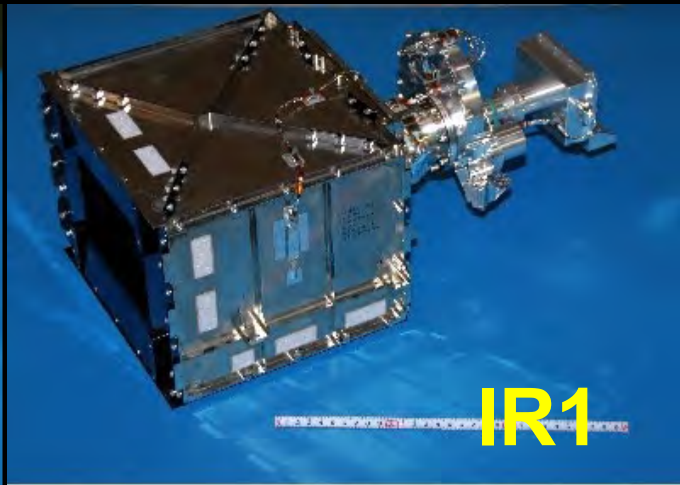

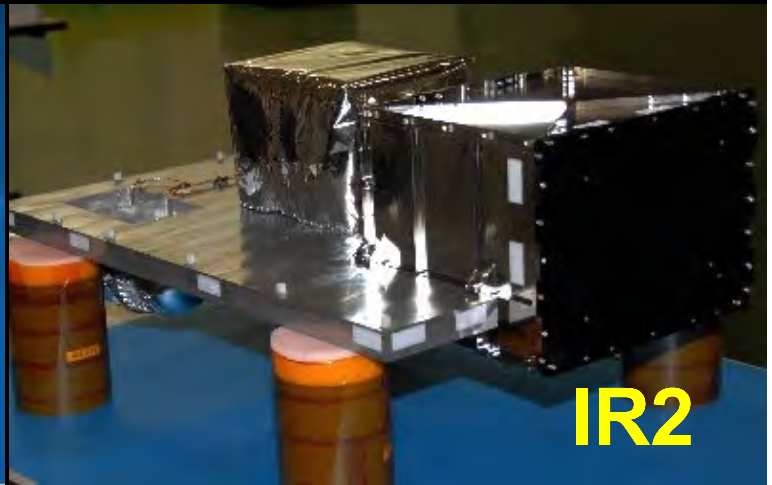

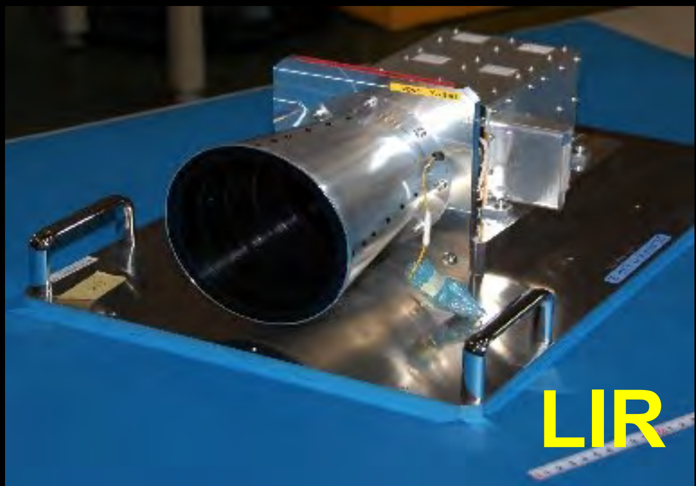

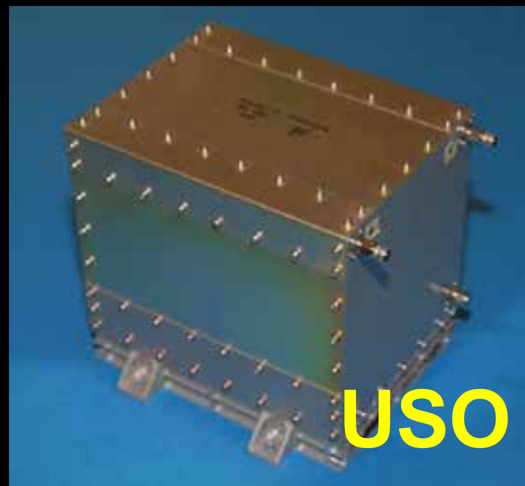

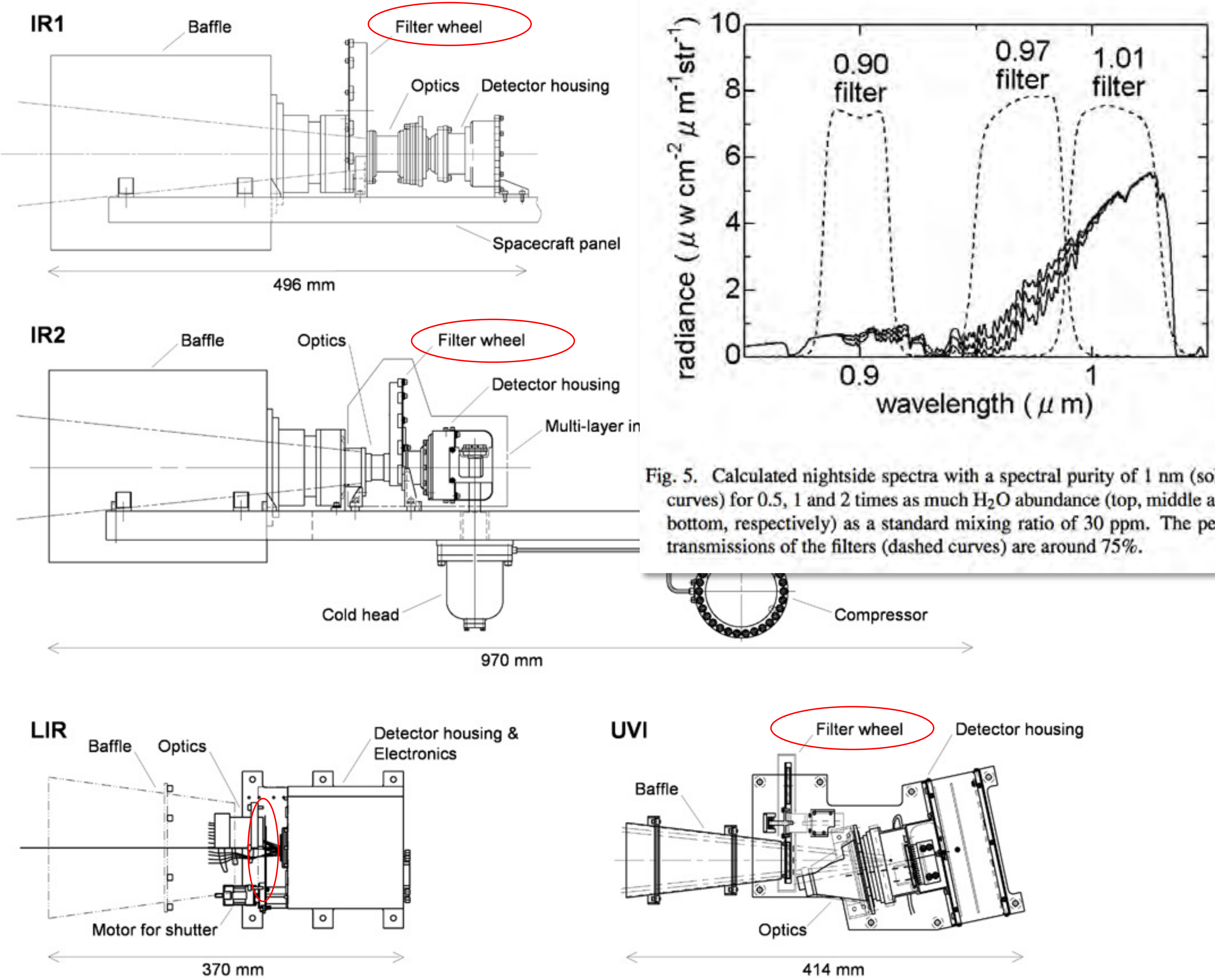

Fig. 5. Calculated nightside spectra with a spectral purity of 1 nm (solid curves) for 0.5, 1 and 2 times as much H_2O abundance (top, middle and bottom, respectively) as a standard mixing ratio of 30 ppm. The peak transmissions of the filters (dashed curves) are around 75%.

Venus seen by Akatsuki

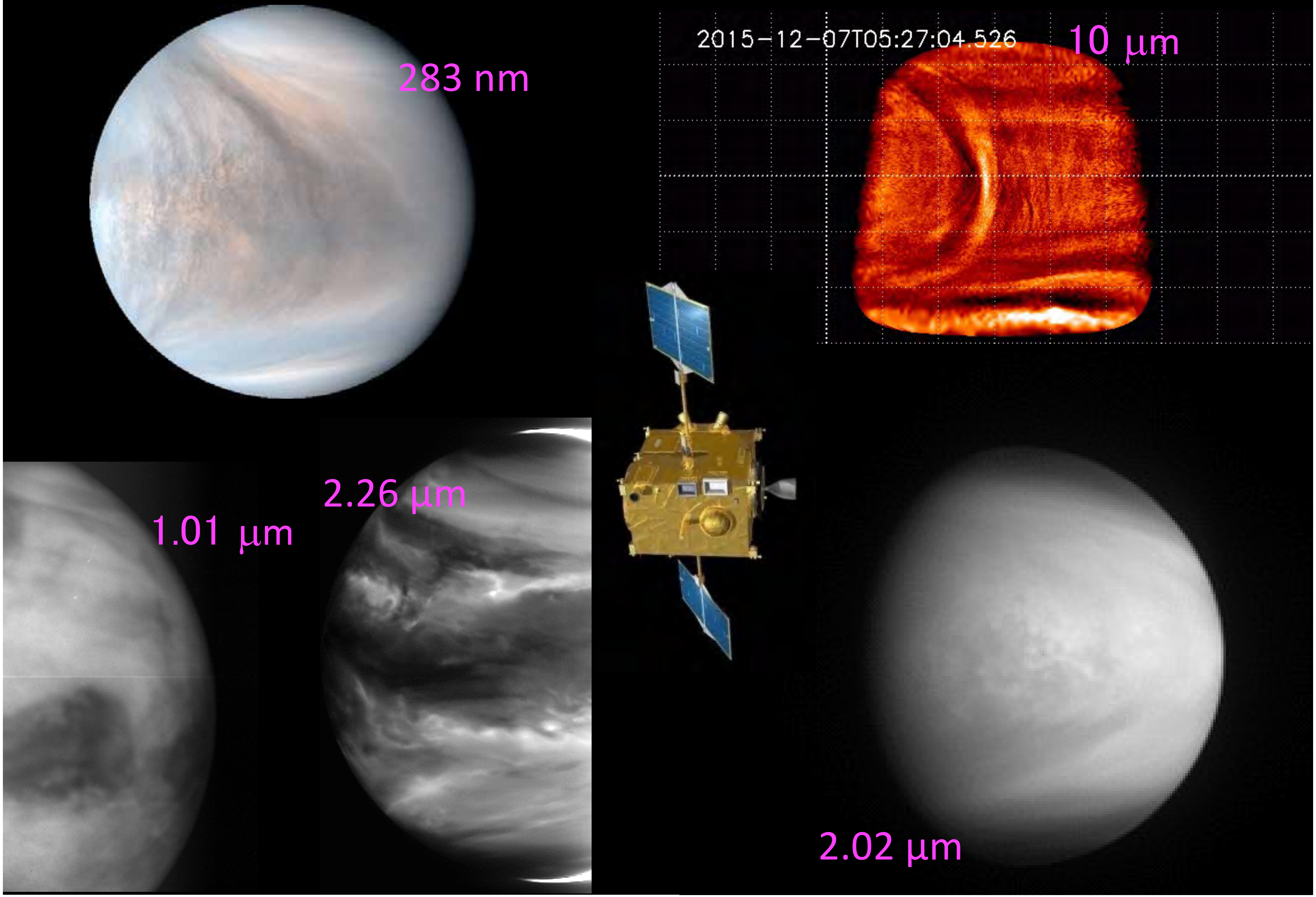

Junocam: Juno's Outreach Camera

Hansen et al. (2014)

Fig. 12 Color filters are bonded directly to the CCD

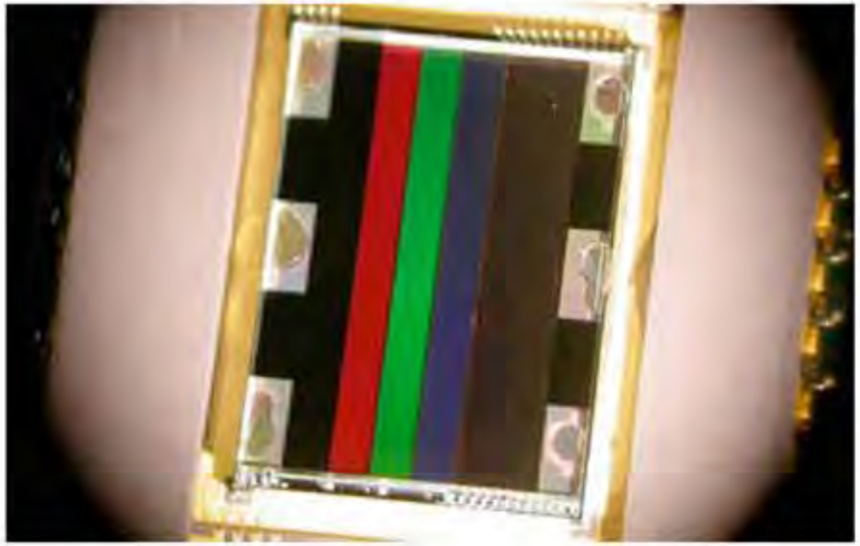

Table 3 Junocam filter characteristics

Band	Blue	Green	Red	Methane
Center wavelength	480.1 nm	553.5 nm	698.9 nm	893.3 nm
FWHM	45.5 nm	79.3 nm	175.4 nm	22.7 nm

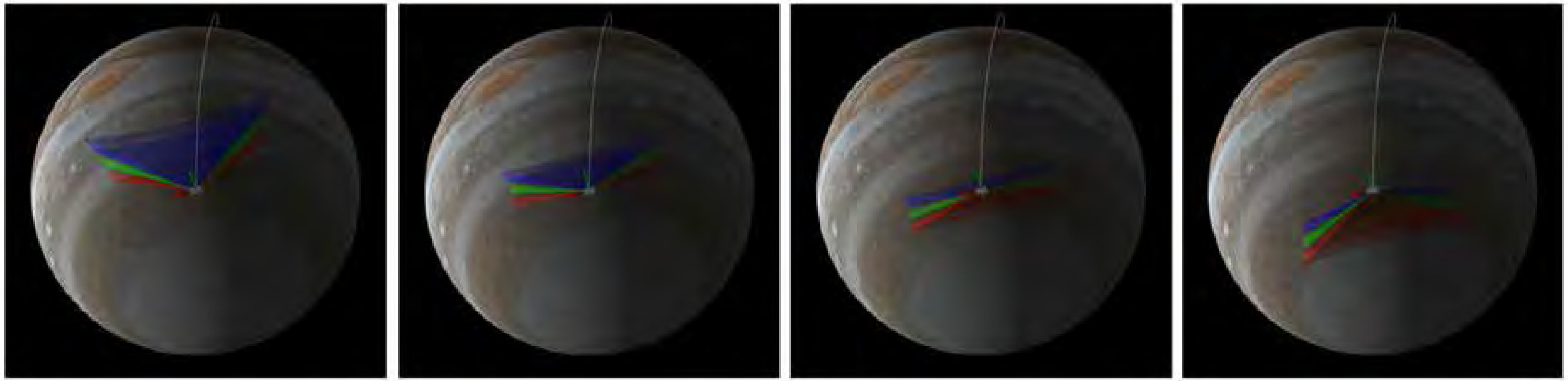

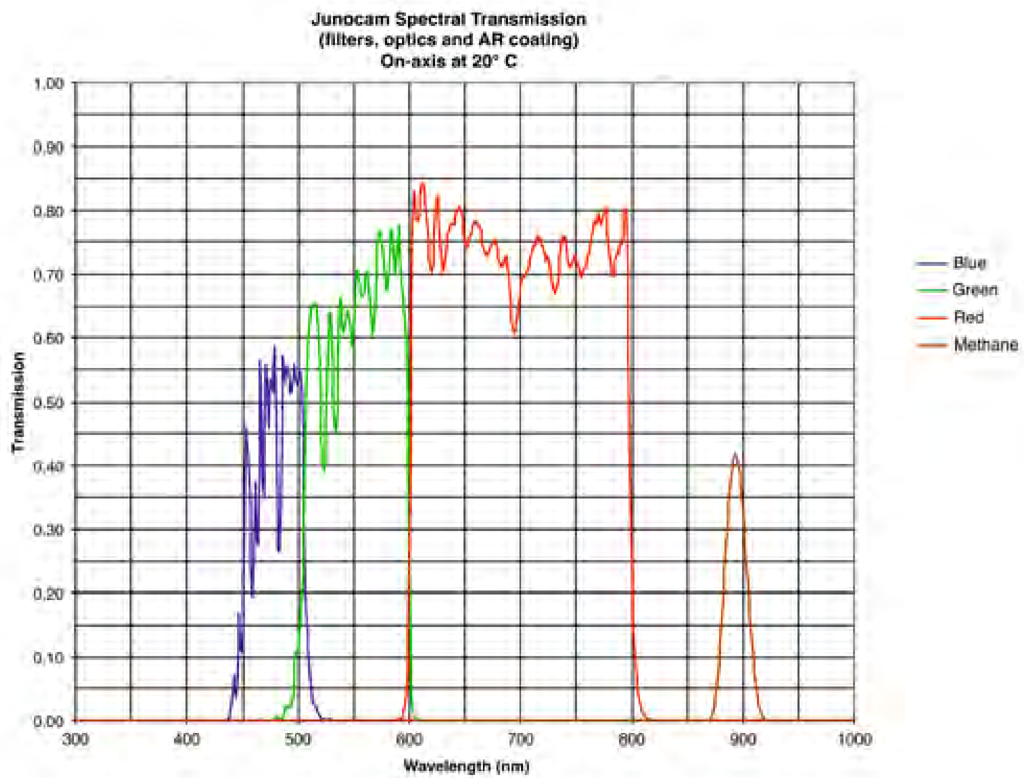

Fig. 13 Bandpasses and transmission are shown for Junocam's four filters

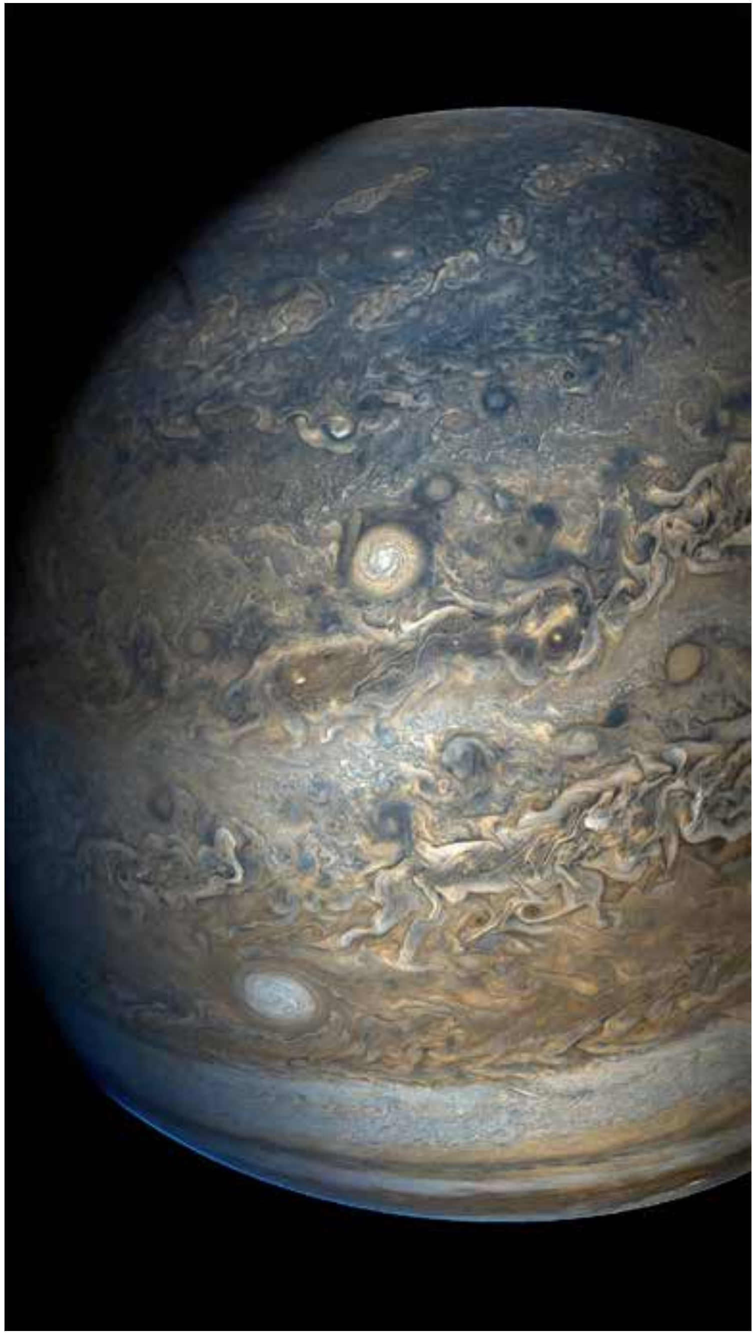

Mars atmosphere observation in MMX mission

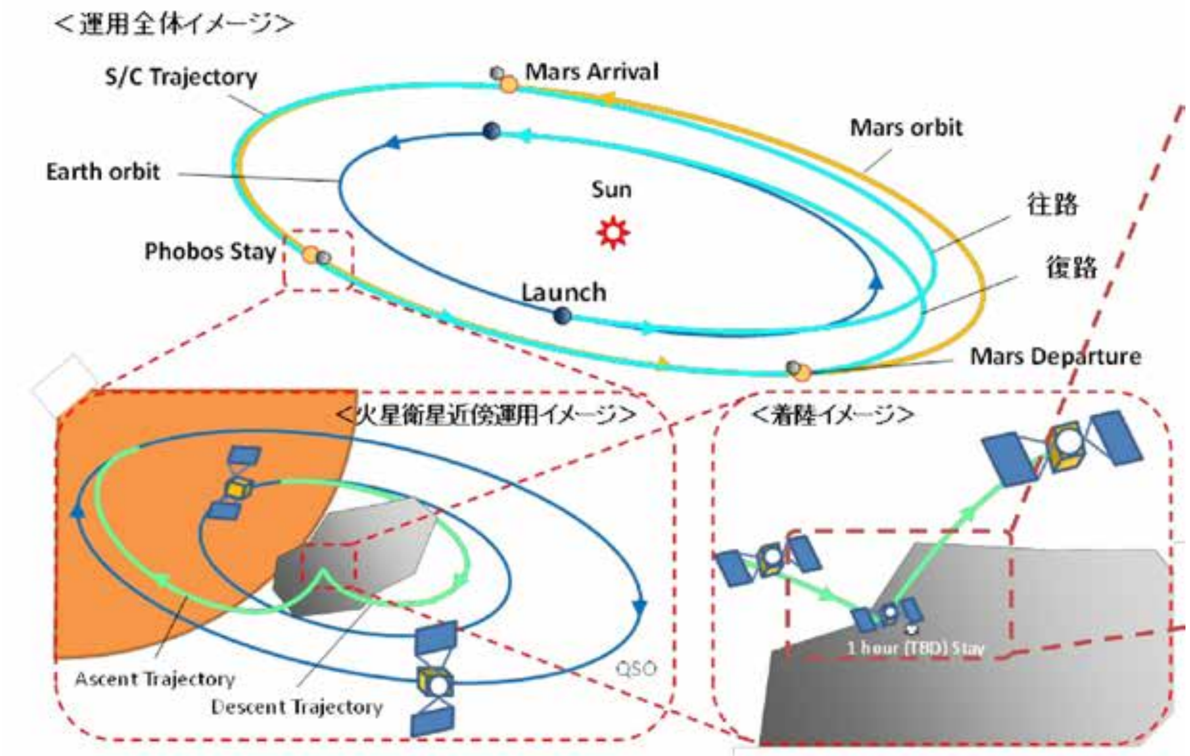

MMX: Martian Moons Exploration

- Mission to Mars/Phobos/Deimos
- Sample return from Phobos
- Three years in Mars orbit
- Target launch year is 2024

Continuous global monitoring from Martian orbit

High-altitude equatorial orbit is a unique platform for atmospheric studies

Ogohara et al. (2022)

Venus images taken by Akatsuki

UV

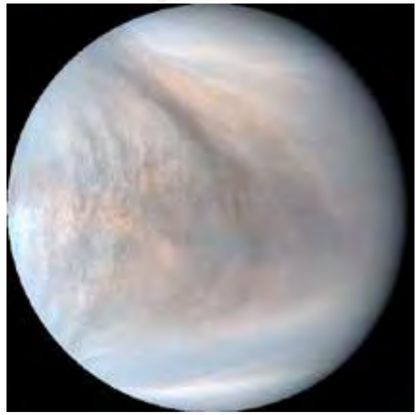

IR

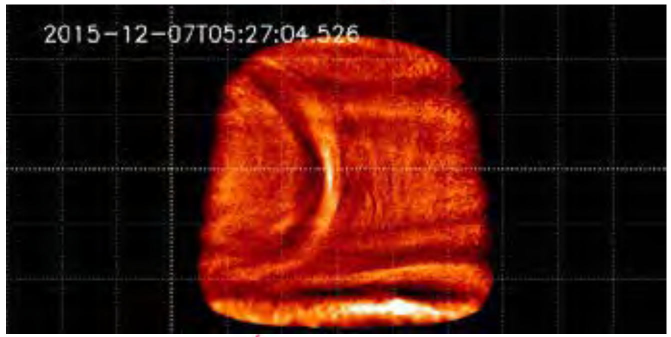

Instruments for Mars atmosphere observation

- **OROCHI** (Kameda et al., 2021)
  - 8 colors are available. 3 colors (480, 650, 950 nm) will be used for Mars observation.
  - 2.5 km/pix (sub S/C) from QSO
- **TENGOO** (Kameda et al., 2021)
  - Panchromatic
  - 35 m/pix (sub S/C) from QSO
- **MIRS** (Barrucci et al., 2021)
  - Push-bloom type spectrometer
  - Spectral resolution: 10nm
  - Spectral bandpass: 0.9–3.6 μm
  - 2.1 km/pix (sub S/C) from QSO

Kameda et al. (2021)

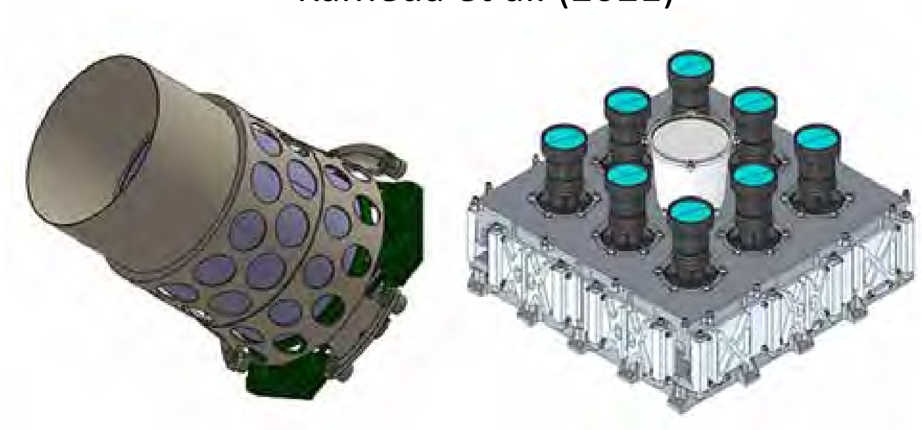

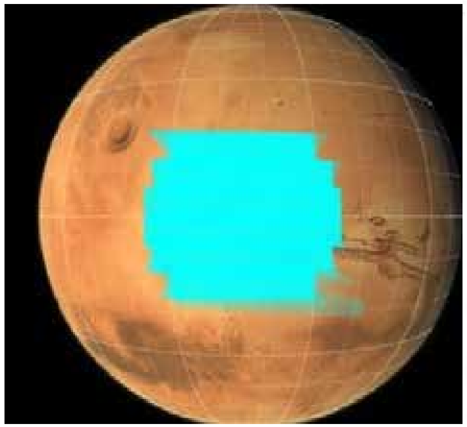

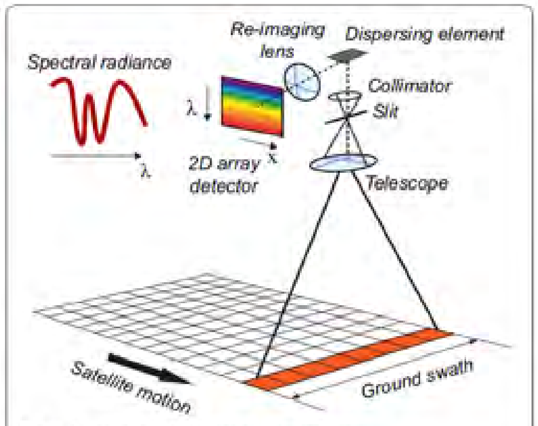

Fig. 4 Scheme for a push-broom spectrometer

Barucci et al. (2021)

Simulated MIRS spectrum

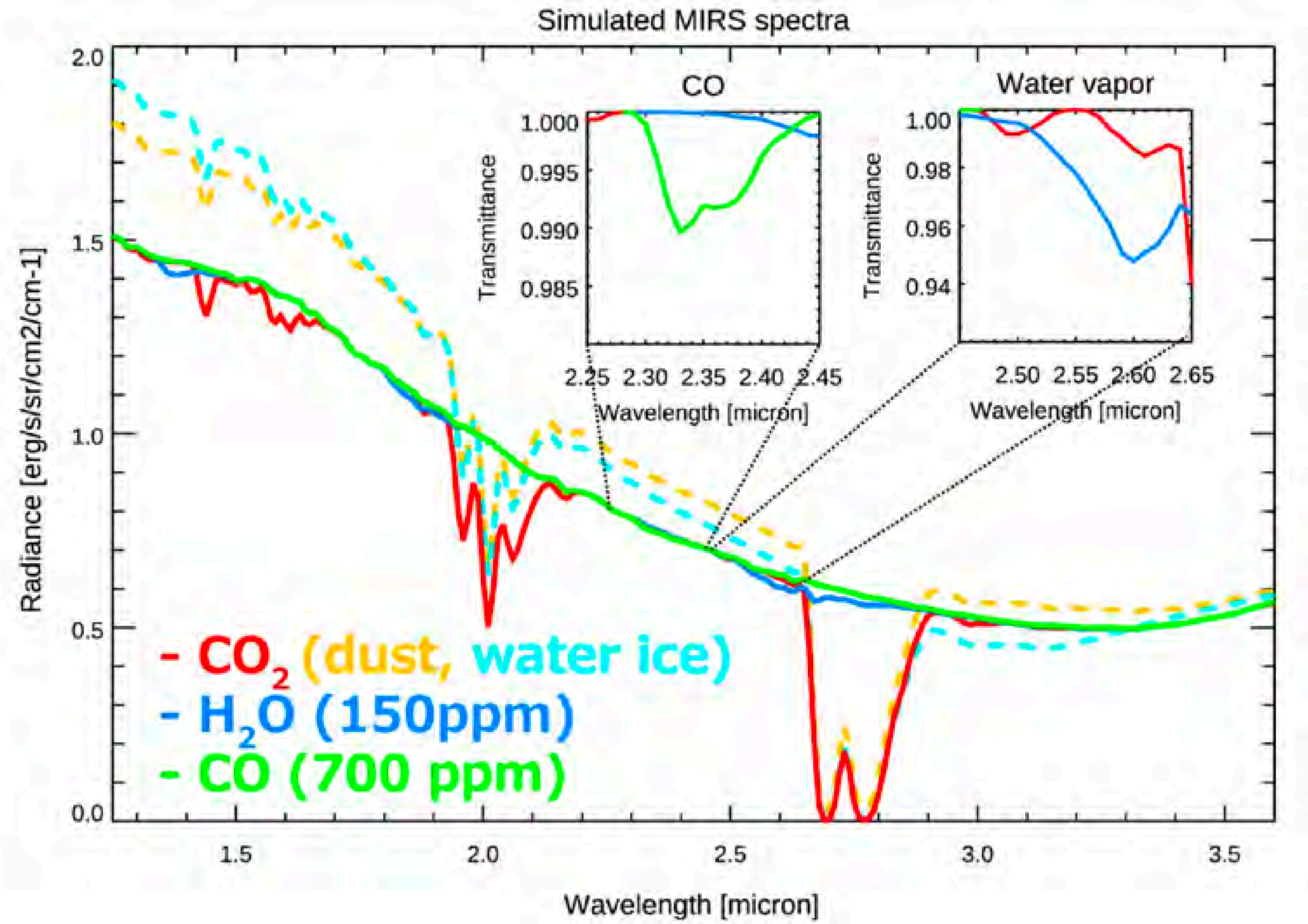

Barucci et al., EPS, 2022

Strategy of Mars atmosphere observation

- High frequency, high spatial resolution, global monitoring of :
  - Dust storms and their rapid development
  - Fine structure of water vapor, water ice cloud, and their local time variation
- Sampling interval = 15 min (OROCHI) or 1 h (MIRS)
- Length of continuous monitoring = 3 h
- (limb viewing) Vertical profiles of water vapor, water ice, and dust